Affinity tag excision strategies for Car9-tagged proteins

Kannan Aravagiri

A thesis
Submitted in partial fulfillment of the
requirements for the degree of

Master of Science

University of Washington
2016

Committee:
François Baneyx
Qiuming Yu

Program Authorized to Offer Degree:
Chemical Engineering

University of Washington

Abstract

Affinity tag excision strategies for Car9-tagged proteins

Kannan Aravagiri

Chair of the Supervisory Committee:
Professor François Baneyx, Ph.D.
Chemical Engineering

The demand for cheap methods to evaluate and purify of proteins is growing especially in the emerging sectors of the biologics industries and in research laboratories. In accommodating this demand for growth, we explore the possibility that the Car9 affinity tag, a silica-binding dodecamer, may provide an inexpensive alternative to the current gold-standard, the hexahistidine tag. Specifically, we show that the Car9 extension, which was previously shown to be functional as a C-terminal affinity tag, supports rapid purification when appended to the N-terminus of proteins, yielding a >85% purity in a manner of minutes. In addition, we demonstrate two novel methods of Car9 tag removal using the outer-membrane protease, OmpT. The first involves the use of OmpT-overproducing *E. coli* cells crosslinked to chitosan microspheres using glutaraldehyde. The second employs a mutated version of purified Ompt that is itself modified with a Car9 tag. We show that the immobilized cells support complete excision of a C-terminal Car9 tag in 24h of incubation with no contaminant formation. These catalytic microspheres are reusable, storable, and show promise for larger scale experiments. An OmpT-Car9 fusion protein refolded from inclusion bodies was also shown to support Car9 tag

cleavage, and removal with silica. However, further experimentation will be required to determine binding affinity of OmpT-Car9 for future purification and retrieval optimization experiments.

Table of Contents

List of Figures

List of Tables

Acknowledgements

I would like to acknowledge those who have helped me greatly during my development of my dissertation and process. I would first like to thank my lab-mates former (Brandon, James, Brian), current (Jessica, Alex, Brittney, Wenlan, Sonja), and Meng Xu, who have been nothing but giving in their knowledge, creative spirit, and aid during my times of need.

I would like to give special thanks to the Dr. Pozzo and her group, especially to David, Yi Ting, and Kiran for letting me use their homogenizer and giving me their time and essential advice on how to progress in my experiments. As well, I have to give thanks to Dr. Berg's group and especially Ed Michor for also letting me use their homogenizer.

I would like to thank my advisor François Baneyx, for giving me the great opportunity to work in his lab, advice and mentorship to grow as a researcher, and for being patient with me during my years here. Additionally, I would like to thank Dr. Qiuming Yu for being ever inspiring me to be curious and to love science in this engineering program.

Finally, I would like to thank my family, the Dr.s Aravagiri and Arunmozhi, for constantly being there and supporting me through my entire life.

Introduction

I. Affinity Tags and the Car9 extension

As the technology to produce recombinant proteins advances especially with progress in genomics and proteomics, the demand for cheap and easy purification strategies has only grown. One such purification scheme, that is extensively used in basic research and biologics production schemes, is the use of affinity tags. These tags are short peptide segments that are fused to the N-or C-terminus of a recombinant protein and bind with high affinity to a ligand or resin [1,2]. Although many affinity tags have been studied (Table 1), new affinity extensions that support faster or cheaper protein purification schemes are desirable. One such tag is the Car9 affinity tag. This dodecapeptide, DSARGFKKPGKR, supports the purification of tagged proteins on silica beads, which are significantly cheaper material than the current gold standard: the nickel-nitroloacetic acid (NTA) resins used for the purification of His-tagged proteins [3]. Coyle and Baneyx previously demonstrated that proteins containing a C-terminal Car9 extension supports efficient protein purification [3]. Here, we demonstrate that the Car9 tag is also functional when appended to the N-terminus of a protein, a more desirable from standpoint of precise tag excision [4,5]. We also introduce two innovative purification schemes for the removal of Car9 extensions to produce native-like proteins.

II. Removal of Affinity Tags

The removal of affinity tags is often necessary to prevent any deleterious effects on protein structure or function and to reduce immunogenicity [6]. A number of methods, therefore, have been developed for tag excision. The two most popular chemical methods include the use of cyanogen bromide in the presence of either hydrochloric acid or formic acid to promote cleavage C-terminal methionine residues or hydroxylamine to induce cleavage between asparagine and glycine residues [7]. These chemical methods are both non-specific in that can cleavage can occur in other portion of the protein, and require harsh reaction conditions such as pH extremes or the use of highly reactive chemicals. The most effective means cleavage of the affinity tag removal involves using a protease that recognizes and cleaves a specific target sequence of amino acids. Protease cleavage for affinity tag removal has been thoroughly studied reviewed (Table 2). The use of endoproteases and exoproteases is most common. Endoproteases such as

TEV protease, Factor Xa, and thrombin, require high ratios of enzyme to protein, and long incubation periods of times for complete excision [4]. Exoproteases or exopeptidases are less commonly used as they are difficult to remove, but unlike common endoproteases, are efficient in removing C-terminal affinity tags [5]. Both types of proteases allow for specific excision under near physiological pH conditions (pH 6 - 8).

Instead of using exo- or endoproteases to excise the Car9 tag from sfGFP -Car9 fusion protein, Coyle and Baneyx found that OmpT, an outer membrane protease, was capable of excisint the Car9 tag with high efficiency and specificity. [3,8].

III. OmpT

OmpT, as shown in Figure 1, is a 33.5 kDA β-barrel that is embedded in outer-membrane of gram negative bacteria. Its active site consisting of Glu-27 and Asp-208 projects towards the growth medium and cleaves substrates between dibasic amino acid residues [9,10]. The aspartate and glutamate residues in the extra-cellular space form a negative pocket flanked by hydrophobic regions further indicating that the efficiency of OmpT increases when the dibasic residues are flanked with hydrophobic residues [11,12,13]. Serine protease inhibitors weakly inhibit OmpT activity, while $ZnCl_2$ and $CuCl_2$ are more effective inhibitors [9,12]. Here, we explore two OmpT-based strategies for inexpensive and effective removal of Car9 tags from partner proteins. The first involves crosslinking OmpT-over producing *Escherichia coli* cells to the surface of chitosan microspheres using glutaraldehyde in order to produce a high-density matrix [Figure 6]. The second involves purifying and using OmpT variant with a modified Car9 for Car9 tag and protease removal [Figure 7].

IV. Chitosan

Substrates for whole cell immobilization should have chemically modifiable surface groups, be inexpensive, and be biocompatible. One such substrate is chitosan, a cellulose polymer consisting of a mixture of β-(1-4)- linked - D-glucosamine and N-acetyl-D-glucosamine monomers, produced by deacetylation of chitin [14] [Figure 2].

Chitosan macromolecules display amine groups, which are accessible to traditional cross-linking agents, such as glutaraldehyde [15]. Chitosan has been used for encapsulation and delayed release of drugs, and for entrapping whole cells into porous bio-catalytic spheres

[15,16,17]. For such applications, whole cells were added to polymeric chitosan dissolved in a dilute solution of acetic acid, and the mixture was either dispensed dropwise into an anionic solution such as 2M sodium hydroxide or tripolyphosphate or crosslinked while dispersed in an oil/water emulsion in order to induce entrapment through ionotropic gelation [16,17,18]. Ionotropic gelation is a method by which anions form salt bridges between positively charged amine groups, polymerizing chitosan into structures [18] [Figure 5]. Here, we chose crosslink whole cells over-producing OmpT onto the surface of chitosan microspheres, produced through ionotropic gelation in a water/oil emulsion, for OmpT to cleave Car9-tagged substrates. Previously, whole cells, fixated with glutaraldehyde, had been cross-linked to chitosan-coated cellulose powder, showing the potential of chitosan as a conduit for whole-cell immobilization for outer-membrane protein activity [19].

V. Glutaraldehyde

Glutaraldehyde, whose structure is shown on Figure 3, is a 5-chained carbon molecule terminated with aldehyde groups. This conformation allows for selective fixation of nucleophilic substrates. By attacking to protein-bound nucleophilic R-groups found on lysine and histidine, glutaraldehyde can covalently couple outer membrane proteins onto a nucleophile functionalized surface, such as chitosan. How glutaraldehyde reacts with these amino acids is still under debate [20]. In addition to crosslinking capability, glutaraldehyde crosslinking often eliminates cell viability, but the issue is not one of concern, since we wish to make use of membrane embedded OmpT and do not need a living biocatalyst [21]. In fact, our ideal scenario relies on the use of immobilized outer membrane with all contaminating cellular contaminants removed. Thus, further processing such as freeze-drying or incubation with cell permeating compounds might be needed to produce the desired cleavage matrix [22].

VI. OmpT purification using Car9 and activation with LPS

Another tag excision scheme would involve adsorbing purified OmpT onto silica beads using a modified Car9 tag that is not prone to autodigestion [Figure 7]. Kramer and coworkers have shown that overexpressed OmpT can be purified from inclusion bodies and activated using lipopolysaccharides (LPS) to produce abundant amounts of functional protease [23]. OmpT and Car9 tag can each be modified to proteolysis or OmpT-mediated cleavage (Hellner and Baneyx

unpublished data) [24] [Figure 7]. Here, we aimed to show a unique affinity tag excision technique by which a variant of OmpT, exhibits a lower propensity to autoproteolysis is fitted with a modified Car9 affinity tag and mixed with a Car9 tagged target protein. In this scheme, the excised tag and OmpT-Car9 are retained on the silica beads while the target protein with a digested tag remains in the supernatant.

First, we demonstrate whole-cell immobilization of SF100 harboring pML19 onto chitosan microspheres as an effective tool for Car9 removal, offering full cleavage within 24h with no additional contaminant formation. Secondly, we demonstrate that OmpT-Car9 is active, capable of Car9 excision, and is removable with silica, but requires modification to increase OmpT-Car9's binding affinity to silica.

Material and Methods

I. DNA manipulations

Plasmid pNC9A was constructed by first inserting a *Nde*I-*Nco*I cassette encoding the Car9 dodecamer, followed by a GGGS linker and a TEV protease site (Figure 4) into the same sites of pET-22b(+) (Novagen). The gene encoding super folder green-fluorescent protein (sfGFP) was next PCR amplified on a *Nco*I-*Hin*dIII fragment using primers 5'-GGGCCATGGGGCGTAAAGGCGAAGAGCTGTTC-3' and 5'-GCCAAGCTTTTATTTGTACAGTTCATCCATACC-3' and inserted into the same sites of pNC9A to yield pNC9A-sfGFP. All DNA manipulations were performed in Top10 cells [Figure 4].

A modified *ompT* gene containing the K216G and G217 mutations that reduce autocatalytic cleavage in loop 4 was created by site-directed mutagenesis of plasmid pML19 using the Quickchange mutagenesis system and primers 5'-CACTATGACCCGAAAGGAAGAATCACTTATCGC- and 5'-CACTATGACCCGAAAGGAAGAATCACTTATCGC-3' [24]. The modified *OmpT* gene was PCR-amplified on a *Nde*I-*Hin*dIII fragment using primers 5'-GGTGGTCATATGTCTACCGAGACTTTATCG – 3' and 5'-GGGAAGCTTAAATGTGTACTTAAGACC-3'. This amplified fragment was digested with *Nde*I and *Hin*dIII restriction enzymes for 5h at 37°C and purified via agarose gel purification. The purified fragment is then cloned into the vector pET24a(+) (Novagen) containing the gene expressing sfGFP-K8H/K11H Car9 to make OmpT K216G/G217 - Car9 K8H/K11H (Hellner and Baneyx unpushblished). This plasmid was called pOmpTC9.

II. Rapid protein purification

For protein expression, plasmid pNC9A-sfGFP was introduced into BL21(DE3) cells and seed cultures (10 mL) were used to inoculate 500 mL of LB medium supplemented with 100 µg/mL carbenicillin. Cells were grown to A600 of 0.4 at 37°C and protein synthesis was induced with addition of 1 mM IPTG. After 6 h of incubation, cells were harvested by centrifugation at 10,000*g* for 10 min, and resuspended in 40 mL of 20 mM Tris HCL pH 7.5

(Buffer A) supplemented with 2 mM EDTA. Cells were disrupted by six round of sonication for 3 min at 30% duty cycle using a Branson sonifier. Lysates were clarified by centrifugation at 10,000*g* for 10 min. The supernatant was then placed in a hot water bath (75° C) for 15 minutes and centrifuged again for 10 min at 10,000 G. This final supernatant (sfGFP-Buffer) was then dialyzed 3 times at 10 volumes of Buffer A [3].

4 g of silica gel (200-420 mesh, 150A pore, Sigma Aldrich) was resuspended in 50 mL of Buffer A and the slurry was placed in a gravity column with an inner diameter of 2.5 cm that is plugged with glass wool and connected to a 30 mL syringe through a plastic two-way valve, as described in [3]. After washing the slurry with 30 mL Buffer A through the bed at least 3 times and until the flow through was clear. Clarified lysate (40 mL) was then dispensed to the top of the bed and the solution was aspired through the bed until the meniscus reached the top of the silica. The slurry/protein mixture was allowed to incubate for 10 minutes for full complexation to occur, and was then washed with 5 bed volumes of Buffer A before being eluted with 75 mL of Buffer B (with 20 mM Tris pH 8.25 ,500 mM lysine). Eluted fractions were then concentrated through centrifugation for 15 min at 3500*g* using a 10 kDA cutoff Amicon ultra centrifugal filter (Millipore). Samples (15 mL) were dialyzed against 5 L of Buffer A at 6°C with 5 buffer exchanges over a period of 48h. Protein purity was 85% as judged by SDS-PAGE analysis after processing and 15 mL of 1.4 mg/mL sfGFP-Car9 was retrieved as determined by bicinchoninic acid (BCA) assay.

For TEV cleavage, 14 μg of purified Car9-sfGFP was incubated with 10 units of the commercial TEV protease, ACTev^{TM,} in a total reaction mixture of 150 μL for 12 -72 hr. 10 μL aliquots were removed at certain time points and analyzed on SDS-PAGE.

III. Simple Characterization of protein-silica interactions using fluorescence depletion assay

Silica gel (Davisil grade 62, 150 Å pore size) in amounts increasing from 5 to 150 mg was transferred to .2 mL mL PCR tubes. Next, 200 μL stock of Car9-sfGFP or sfGFP-Car9 at of 2.5 μM was added to each tube. After 1h with gentile agitation, the supernatant was removed and fluorescence was quantified at 520 nm following excitation at 485 nm using SpectraMax microplate reader (Molecular Devices).

IV. Chitosan microsphere preparation using ionotropic gelation

The protocol is adapted from Zamora, Natesan, & Christy, 2012 [42]. Chitosan (medium molecular weight, purchased from Sigma #448877) is first dissolved in 2% vol/vol acetic acid to make a 2.5% wt/vol solution. 10 mL of the solution was added to a 1:2 1-octanol/paraffin oil mixture supplemented with 5% wt/vol Span 85 emulsifier (Sigma) in a beaker. The mixture was subjected to 2000 rpm agitation using a Ross homogenizer and ~1000 rpm agitation using a magnetic stirring bar, spinning in the opposite direction. After 1 h of emulsification, 1 % wt/vol KOH in butanol is added in 1.5 mL boluses every 15 min for 4 h for a total of 24 mL. The oil phase was removed and discarded and the chitosan microspheres were washed repeatedly using acetone (10 mL) and heptane (10 mL) until all residual oil is removed. The microspheres were dried overnight in a fume hood and soaked in 20 mL of water for at least 4 h before crosslinking.

V. Fixation and crosslinking of sf100 onto chitosan microspheres

SF100 cells (F- *ΔlacX74 galE galK thi rpsL (strA) ΔphoA (PvuII) Δ(OmpT- entF*) [9] harboring pML19, a plasmid that encodes a chromosomal DNA segment encompassing the OmpT gene, were grown in 50 mL of LB medium supplemented with 100 µg/mL carbenicillin for 3h at 37°C. The optical density of the cultures was adjusted to A_{600}~1 using LB (dry cell weight of ~ 1 mg/mL) and cells were harvested by centrifugation at 3000*g* for 20 min and washed twice with 20 mL of phosphate buffer saline (PBS, 10 mM PO_4^{-3}, 137 mM NaCl, 2.7 mM KCL pH 7.5). Cells were resuspended in 1 mL PBS and added to .2% v/v glutaraldehyde in PBS for a final volume of 40 mL which was incubated overnight under constant agitation in an ice bath [19]. Crosslinked cells were harvested by centrifugation at 3000*g* for 20 min, washed twice with PBS to remove unreacted glutaraldehyde, and resuspended in 1 mL of PBS. Aliquots (100-500 µL) of crosslinked cells were added to 0.2 g of chitosan microspheres prepared as above and the mixture (2 mL) was incubated on a rotary shaker at 64 rpm at room temperature for 72 h.

VI. Excision of the Car9 tag using cell-coated chitosan microspheres

Cell-coated chitosan microspheres (10 µL) were added to purified sfGFP-Car9 or Car9-sfGFP (12 µg) and left to incubate on a rotary shaker for .5 to 24 hr. Samples were subjected to centrifugation at 5000g for 3 min and the supernatant was recovered for SDS-PAGE analysis. Cell-coated chitosan microspheres were washed thoroughly and stored at 4°C.

VII. Production of OmpT-Car9

For protein expression, plasmid pOmpTC9 was introduced into BL21(DE3) cells and seed cultures (25 mL) were used to inoculate 500 mL of LB medium supplemented with 50 µg/mL kanamycin. Cells were grown to A600 of 0.4 at 37°C and protein synthesis was induced with addition of 1 mM IPTG. After 6 h of incubation, cells were harvested by centrifugation at 10,000 g for 10 min, and resuspended in 40 mL of 50 mM Tris HCL pH 7.5 (Buffer C) supplemented with 40 mM EDTA. Cells were disrupted by six round of sonication for 3 min at 30% duty cycle using a Branson sonifier. Lysozyme was added to a concentration of .1 mg/mL and let to sit on ice for 1 hr. The lysate is then sonicated once and centrifuged for 10 min at 1500*g* to remove any un-lysed cells, and the supernatant is given a hard spin of 10,000*g* for 20 min to retrieve the inclusion bodies (IB). Inclusion bodies were washed by resuspending the cell pellet with 50 mM Tris pH 8.1 supplemented with 1 mM EDTA, sonicating once, and centrifuging at 10,000*g* for 20 min. This was done twice. Washed inclusion bodies were then dissolved in 10 mL of 8M urea pH 8.3 supplemented with 50 mM glycine overnight on ice with agitation from a rotary shaker. 10 mL of chilled 20 mM Tris pH 7.5 supplemented with 50 mM dodMe_2NPrSO_3 (N-dodcyl-N, N,-dimethyl-1-ammonio-3-propanesulphonate from Sigma) was added to the dissolved inclusion bodies and kept on ice for an additional 1 hr. This solution was then spun down at 2000*g* for 10 min to remove any unfolded product. The supernatant was then dialyzed against 10 volumes of 20 mM Tris pH 7.5 supplemented with 10 mM dodMe_2NPrSO_3 three times to refold OmpT-Car9. Protein concentration was quantified using BCA assays (2 mg/mL total) and purity though SDS-Page with imageJ analysis (80% of total protein was OmpT-Car9). Protocol was adapted from Kramer et. Al. [21]. OmpT-Car9 solution was then incubated with 1 µg/mL lipopolysaccharides (LPS) from Escherichia coli 0111: B4 purified by phenol extraction method (Sigma). This solution was then dialyzed three times over the course of

24h against 4 L of Buffer A to remove the detergent [23, 24]. Final volume was 15 mL of purified protein.

For tag removal experiments displayed on Figure 16 and 17, 2 µg and 1 µg of OmpT-Car9, respectively, were inserted into 50 µL of 10 µM sfGFP-Car9 and allowed to incubate from 1-24h. Aliquots of 20 µL were removed and prepared for SDS-PAGE gel. The other 30 µL were incubated with 10 µL of silica slurry for 15 minutes. Afterwards, 20 µL aliquots were removed for SDS-PAGE analysis.

For tag removal experiments as displayed on Figure 18, 1-50 µL of 1 mg/mL OmpT-Car9 was added to 100 µL of 10 µM sfGFP-Car9 and suspended with 1X PBS for a total volume of 150 µL. After 4h of incubation at RT, 30 µL of reaction mixture was aliquoted and prepared for SDS-PAGE analysis while the other 120 µL were incubated with 30 µL of silica gel slurry (70-230 mesh, 6 nm pore size, Sigma). This was allowed to incubate for an additional 15 minutes before retrieving 30 µL aliquots of the supernatant for SDS-PAGE analysis. Tag removal

Results and Discussion

I. N-terminal Car9 purification scheme

The Car9 affinity tag (DSARGFKKPGKR) has been shown to bind efficiently to silica [3]. As previously described, positively charged and hydrophobic residues on the Car9 sequence mediate binding through silica's hydroxyl/ silanol and siloxane groups, respectively [8]. Fusion of the Car9 tag to the N terminus of proteins could offer maneuverability and open up strategies for efficient tag removal [3,4]. In order to determine the effectiveness of the N-terminal Car9 tag and to provide a mode for endoproteolytic cleavage, we constructed a plasmid containing Car9 tag, GGGS linker, and a tobacco etch virus (TEV) cleavage site in pET-22b(+), creating pNC9A. Genes encoding sfGFP, a robust GFP variant of the folding reporter GFP which includes six mutations: S30R, Y39N, N105T, Y145F, I171V, and A206V, were cloned into pNC9A using *Nco*I and *Hind*III resctrictions sites to construct Car9-sfGFP [45] (Figure 4). In order to determine binding efficiency of the N-terminal tag in comparison to the C-terminus tagged protein, fluorescence depletion assays were performed to compare two variants [3]. A fixed amount of sfGFP-Car9 and Car9-sfGFP (15 μg) was added to increasing loads of silica -gel and incubated for 1h[3]. The fluorescence in the remaining supernatant was then quantified using a fluorescence plate reader. Analysis of the fluorescence retrieved from the supernatant suggest that both variants bound to silica with similar affinity, attaining 98% purity of Car9-sfGFP from an 85% pure load, following the same rapid-purification technique Coyle had described previously [Figure 9][3].

Endoproteases work most efficiently for N-terminally tagged fusion proteins and leave fewer amino acids on the newly cleaved N-terminal side as compared to the C-terminal side of the scissile bond [Table 2] [4,5]. By placing the TEV site between the Car9 tag and the native protein, we demonstrate the cleavage the Car9-sfGFP fusion protein to its native sfGFP state with incubation with the commercial TEV protease, AcTEV™ (Figure 10). AcTEV™ protocols detail that 10 units of protease can cleave 20 μg of fusion protein (Thermofisher). Instead, AcTEV™ protease required upwards of 48h to fully excise the Car9 tag from 14 μg Car9-sfGFP (Figure 10).

These results show that the Car9 tag is a versatile purification peptide tag that offers similar binding to silica when fused to the N and C-terminus of proteins. Furthermore, N-terminally tagged Car9-fusion proteins offers the advantage to engage in further processing using endoproteolytic cleavage for tag removal, reducing any interference from the Car9 tag in future uses.

II. Chitosan microsphere formation

In order to provide a structure to accommodate a high-density matrix of OmpT-overproducing *E.coli* for Car9 cleavage, chitosan microspheres were generated through a process of ionotropic gelation using a water/oil emulsion, inspired by Zamora and coworkers' [42].

Briefly, 2.5% aqueous chitosan was added to a 1:1 paraffin oil/octanol solution supplemented with 2 and 5% w/v Span 85. This mixture was agitated 2000 rpm with a magnetic stir bar spinning at 1000 rpm in the opposite direction to prevent aggregation at the bottom of the reaction container. After 1h of emulsion, 1% w/v KOH was added in small boluses of 4 mL every 15 minutes for 4h [42,44]. The formed chitosan microspheres were then cleaned with acetone and hexanes before drying. This ionotropic gelation method produced chitosan microspheres from 50-150 μm in diameter (>80%) with minor aggregates [Figure 11] [41].

Previous methods from Lim et. al. used 2% w/v Span 85 for chitosan microsphere formation [44]. However, experiments using 2% wt/vol Span 85 provided mostly aggregate formations of combined spheres rather than distinct spherical structures incurring limitations on surface area and furthermore crosslinking sites (Figure S6). Increasing to a 5% wt/vol Span 85 showed decrease in spherical aggregates, and produced larger and more distinct spherical formation [Figure 11]. By decreasing aggregate formation, we increase the surface area of the individual chitosan particles, allowing for increased opportunity for crosslinking with *E.coli*. Further studies in optimizing the concentration or type of emulsifier to reduce aggregate formations may be necessary.

Studies on ionotropic gelation in an emulsion had used an aqueous anionic solution (sodium hydroxide) added in boluses and in a slow, constant fashion (e.g. using a peristaltic pump) [43,18]. In our hands, this approach gave rise to uneven particles or extremely large aggregates (5-10 cm) of gelled chitosan [Figure S1]. This is likely due to the uneven distribution

of crosslinker when added into the oil phase causing portions of the emulsified chitosan to crosslink. The uneven distribution of polymerized chitosan and aqueous chitosan may have caused destabilizing effect by which partially polymerized chitosan descended into the aqueous phase of the mixing solution, creating aggregates of amorphous gellated chitosan within basic aqueous solution [44]. Instead, the approach described by Zamora and coworkers uses an anionic crosslinker soluble in organic phase of the emulsion process [42]. The crosslinker is able to distribute evenly, allowing for crosslinking to occur throughout the emulsion simultaneously. Though some aggregate formation occurred as combined spheres, most of the microspheres generated were formed as distinct structures allowing for complete crosslinking to be possible. It is possible that aggregate formation and time required for microsphere formation may be reduced by optimizing the time of additions or by increasing or decreasing the wt% of KOH, but this optimization was not provided here.

Another method in creating chitosan microspheres by ionotropic gelation involved slowly dropping chitosan though a 25-guage needle into a 25 mL container of 2 M sodium hydroxide [17]. When we tried this approach, aqueous chitosan droplets would instantaneously gel once added and could be filtered for further processing. However, droplets could reach to 1-2 mm in diameter, and were too large for efficient crosslinking. Increased relative surface area/volume ratio was required for increased crosslinking efficiency with *E. coli*. Therefore, micron-sized spheres were desired. This led to the use of the current emulsion technique which produced micron sized chitosan spheres, an efficient and stable apparatus for whole-cell immobilization.

Though many factors such as emulsifier type and concentration, crosslinker addition rate, or oil phase type may be optimized to produce more uniform microspheres, the current technique provided a stable substrate for whole-cell crosslinking for OmpT cleavage.

III. Glutaraldehyde fixation and crosslinking of SF100 harboring pML19

In using glutaraldehyde, we aimed to functionalize the side chains of surface exposed lysine and arginine amino acid side chains with aldehyde groups in order to provide a means to crosslink whole cells onto chitosan's nucleophilic amine groups [Figure 3]. Chitosan microsphere producing through ionotropic gelation maneuvers chitosan such that there are free amine groups available at the surface. The free amino groups may be determined using a

trinitrobenzenesulfonic acid assay in order to optimize the chitosan microsphere procedure for increased crosslinking efficiency, but future work is required [44].

As shown on Figure 12, SF100 cells harboring pML19 were fixated with 0.2% glutaraldehyde and furthermore, successfully crosslinked onto chitosan microspheres. As Freeman and coworkers had shown previously, .2% provided enough aldehyde functionalization to occur on the surface-exposed lysine and arginine residues of the cell for efficient covalent crosslinking to occur [19]. Overall, each chitosan microsphere contained highly dense matrix of SF100 cells of around 20 cells per 10 μm^2. Based on the range of chitosan microsphere diameters, we can extrapolate there are 7, 000-100,000 cells per individual chitosan sphere. These catalytically active particles, with interference from mass transfer limitations, was used for Car9 excision.

IV. Car9 excisions using immobilized whole-cells harboring pML19

Figure 13 shows that SF100 (pML19) cells cross-linked to chitosan microspheres (CMSF) could be successfully used to cleave the Car9 tag present on the C-terminus of sfGFP using 1 mg of dry chitosan microspheres and 12 μg sfGFP-Car9 [Figure 13]. Two proteolytic products were detected and the intermediate species disappeared over time to the profit of a product migrating at the position of untagged sfGFP (Fig. 13 lanes 5-8). The presence of these species was previously observed (Coyle) and was explained by the presence of two KK OmpT cleavage sites at the proteins C-terminus (along with a terminal KR site: Figure 15 blue arrows). However, Dekker et. al. [12] have reported that a cleavage at RG (red arrow) is more likely based on the fact that the residues at positions AR*GF and YK*KL are considered favorable cleavage substrates and the expected molecular mass of the removed fragment (.98 and 1.8, respectively) are more similar to the results of Fig. 12. Further analysis by mass spectrometry will be necessary to confirm this hypothesis. Our data suggests that immobilized cells cleave the Car9 tag and linker from the C-terminus of sfGFP and that 24h is sufficient for recovering native protein under our experimental conditions.

One of the advantages of our system is that the immobilized cells can be removed by sedimentation and stored up to several weeks at 4° C without any noticeable change or depletion in cleavage capacity [Figure 15]. Further methods of removal (e.g. filtration) for CMSF retrieval after cleavages may be studied for larger scale procedures. This contrasts to other

protease protocols which must undergo an additional purification process which increases the time and cost of affinity tag removal.

The use of immobilized cells showed no noticeable contamination from *E. coli* host proteins as analyzed by SDS-PAGE gel [Figure 13]. Most of the experiments done using the CMSF were done weeks after crosslinking, and yet there were no signs of lysis or having lysis-products in solution [Figure 13 and 15]. Coyle et. al.'s protocol of tag removal showed unwanted contamination [3]. Freeman and coworkers [20] had shown previously that glutaraldehyde can be used to both significantly limit cell viability in solution and drastically increase cell integrity and thermal stability. Incubation of whole-cells in glutaraldehyde limited the contamination within the system as well as stabilized the cell for long-term use. In addition, further studies on the effects of OmpT from glutaraldehyde fixation may be required to optimize this procedure.

Long-term studies will be required to further delineate the advantages of this process. In addition, introducing substitutive OmpT digestion sites for improved excision efficiency may be the next step for achieving better specificity and efficiency [11].

In summary, we have shown an approach to excising Car9 affinity tags using OmpT-overproducing cells immobilized on chitosan microspheres, which does not introduce contamination and are storable.

V. Ompt-Car9 production

An alternative to the use of whole cells, is to use an immobilized (or affinity removable) OmpT protease, which eliminates the possibility of host protein contamination as in the previous approach.

It has been shown that OmpT can be refolded from inclusion bodies [23] The refolded product is however susceptible to autoproteolysis, and this was circumvented using a G216K/K217G mutation that reduces OmpT activity by 30% compared to wild-type OmpT [23]. Here, we constructed a C-terminally Car9-tagged derivative of OmpT that contains the G216K/K217G mutation.

A total of 24 mg of refolded OmpT-Car9 was retrieved from a 500 mL culture after 6h of induction from a pET system. Isolated inclusion body fractions were approximately of 80% purity according to ImageJ analysis of SDS-Page [Figure 15]. The refolded protein mixture was then incubated with 1 μg/mL lipopolysaccharides (LPS) overnight at 4°C for activation [22]. A position around 30 kDa, or ~5 kDa less than OmpT-Car9, was noticed to have increased in concentration after LPS treatment [Figure 15 red arrow]. This product is likely to be the folded OmpT-Car9 as seen by the primary band migration between denatured and native products on SDS-Page [Figure S5]. This difference in migration has been reported before by Kramer and coworkers [24]. Un-boiled samples of OmpT displayed a faster migration than that of boiled OmpT. As well, high molecular mass products [blue arrow Figure S5], which are contributed to complexes of OmpT to LPS in the un-boiled sample, were absent after boiling [24].

VI. OmpT-Car9 activity and binding

Refolded OmpT-Car9 in solution was activated by incubation with LPS and immediately used in cleaving sfGFP-Car9. 2 μg of OmpT-Car9 was incubated with 50 μL of 10 μM sfGFP-Car9 for 3-24 hrs. The results as shown on Figure 16 revealed successful cleavage of the C-terminal Car9 tag from sfGFP with the same digestion pattern as discussed on chapter IV. In order to remove the OmpT-Car9, the reaction mixture was incubated with 10 μL of silica slurry or 60 mg of silica gel for 15 minutes and the supernatant was collected after centrifugation. As seen on Figure 10, OmpT-Car9 and sfGFP-Car9 was not properly bound to the silica after incubation, which is especially pronounced in lanes D1 and D2 of Figure 16. This was likely due to the detergent involved in the refolding process that caused the decrease in binding efficiency. Initial cleavage experiments were done using OmpT-Car9 in refolding buffer, 20 mM Tris pH 7.5 supplemented with 10 mM dodMe_2NPrSO_3, a zwitterionic detergent. Because it is well known that zwitterionic detergents such as CHAPES is used to remove contaminants and to prevent binding onto affinity tag resins such as nickel-NTA, OmpT-Car9's binding capacity may be reduced due to the zwitterionic detergent in solution [43]. With dodMe_2NPrSO_3 having a CMC of 2-4 mM with an average micellar molecular weight of 18,500, this detergent was removed. After dialyzing against 4 L of 20 mM Tris pH 7.5 three times over the course of 24h, Car9 binding increased with no significant reduction of OmpT activity [Figure 17]. In a 24-hr period, 1 μg of OmpT-Car9 was capable of excising the majority of the Car9 tag from sfGFP

[Figure 17]. In addition, the OmpT-Car9 was removed with incubation with 10 μL silica slurry (~6 mg silica gel). SDS-PAGE analysis on Figure 18 demonstrates some limited binding of OmpT-Car9 especially between lanes D1 and D2, for which further experimentation regarding the binding affinity of OmpT-Car9 may be required.

In summary, we demonstrate a method by which OmpT-Car9 is able to cleave a Car9-tagged fusion protein and furthermore be retrieved with silica gel.

However, recognizing that OmpT-Car9 does not bind as effectively to silica than sfGFP-Car9, optimization will be required in purifying OmpT-Car9 to enable a rapid-purification scheme [Supplementary VIII]. As well, further studies determining an optimal position of the Car9 tag and LPS concentration to keep maximum activity and binding affinity is necessary to increase the efficiency of this process.

Conclusion

In conclusion, we have demonstrated a novel approach to Car9 excision using immobilized OmpT-overproducing SF100 cells crosslinked onto chitosan. The versatility and reusability of the biocatalyst offers a modality for affinity tag removal post-purification. We have demonstrated the versatility of the Car9 tag, which can be positioned to both C and N-terminus of proteins without affecting purification. Finally, we found that OmpT-Car9 can be produced in large yields as inclusion bodies (24 mg per 500 mL culture) and refolded to its active state using the procedure from Kramer et. al. OmpT-Car9 was also able to bind to silica allowing for the removal of the protease from the target protein. Further experiments will be needed to determine the binding affinity of OmpT-Car9 onto silica for purification and OmpT-Car9 retrieval experiments.

References

1. Young , C. L., Bitton , Z. T., & Robinson, A. S. Recombinant protein expression and purification:. *Biotechnology Journal*. 2012, 7.5, 620-634.
2. Lichty, Jordan J., Joshua L. Malecki, Heather D. Agnew, Daniel J. Michelson-Horowitz, and Song Tan. "Comparison of Affinity Tags for Protein Purification." *Protein Expression and Purification* 41.1 (2005): 98-105. Web.
3. Coyle, Brandon L., and François Baneyx. "A Cleavable Silica-binding Affinity Tag for Rapid and Inexpensive Protein Purification."*Biotechnol. Bioeng. Biotechnology and Bioengineering* 111.10 (2014): 2019-026. Web.
4. Arnau, José, Conni Lauritzen, Gitte E. Petersen, and John Pedersen. "Reprint Of: Current Strategies for the Use of Affinity Tags and Tag Removal for the Purification of Recombinant Proteins." *Protein Expression and Purification* (2011): n. pag. Web.
5. Waugh, David S. "An Overview of Enzymatic Reagents for the Removal of Affinity Tags." *Protein Expression and Purification* 80.2 (2011): 283-93. Web.
6. Terpe, K. "Overview of Tag Protein Fusions: From Molecular and Biochemical Fundamentals to Commercial Systems." *Appl Microbiol Biotechnol Applied Microbiology and Biotechnology* 60.5 (2003): 523-33. Web.
7. Andreev, Y. A., Kozlov, S. A., Vassilevski, A. A., & Grishin, E. V. Cyanogen bromide cleavage of proteins in salt and buffer solutions. *Analytical Biochemistry*, 407.1 (2010): 144-146.
8. Coyle, B. L. (2014). Solid-binding Proteins for Modification of Inorganic Substrates. Dissertation of University of Washington.
9. Baneyx, F., & Georgiou, G. In Vivo Degregdation of Secreated Fusion Proteins by the Eschrichia coli Outer Membrane Protease OmpT . *Journal of Bacteriology*, 172.1 (1989) :491-494.
10. Hritonenko, V., & Stathopoulos, C. Omptin Proteins: An Expanding Family of Outer Membrane Proteases in Gram-negative Enterobacteriaceae (Review)". *Molecular Membrane Biology* , 24.6 (2007): 395-406.
11. McCarter, J. D., Stephens, D., Shoemaker, K., Rosenberg, S., Kriscch, J. F., & Georgiou, G. Substrate Specificity of the Escherichia Coli Outer Membrane Protease OmpT. *Journal of Bacteriology*, 186.17 (2004): 5919-5925.
12. Dekker, N., Cox, R. C., Kramer, A., & Egmond, M. R. Substrate Specificity of the Integral Membrane Protease OmpT Determined by Spatially Addressed Peptide Libraries. *Biochemistry*, 40.6 (2001): 1694-1701.

13. Vandeputte-Rutten, L., Kramer, R. A., Kroon, J., Dekker, N., Egmond, M. R., & Gros, P. Crystal structure of the outer membrane protease OmpT from Escherichia coli suggest novel catalytic site. *EMBO J*, 20.18 (2001). 5033-5039.

14. Kas, H. S. Chitosan: Properties, preparations, and application to microparticulate systems. *Journal of Microencapsulation*, 14.6 (1997): 689-711.

15. Sinha, V., Singla, A., Wadhawan, S., Kaushik, R., Kumria, R., Bansal, K., & Dhawan, S. Review: Chitosan microspheres as a potential carrier for drugs . *International journal of pharmaceutics*, 274.1-1 (2004): 1-33.

16. Bagherinejad, M., Korbekandi, H., Tavakoli, N., & Abedi, D. Immobilization of penicillin G acylase using permeabilized Escherichia coli whole cells within chitosan beads. *Research in Pharmaceutical Sciences*, 7.2 (2012) : 79-85.

17. Nomanbhay, S. M., & Hussain, R. Immobilization of Escherichia coli Mutant Strain for Efficient Production of Bioethanol from Crude Glycerol. *Journal of Applied Sciences*, 15 (2015):415-430.

18. Patil, P., Chavanke, D., & Wagh, M. A Review of Ionogtropic Gelation Method: Novel Approach for Controlled GAstroretentive Gelispheres. *International Journal of Pharmacy and Phamaceutical Sciences*, 4 (2012): 27-32.

19. Freeman, A., Abramov, S., & Georgiou, G. Site-Protected Fixation and Immobilization of Escherichia coli Cells Displaying Surface-Anchored β-lactamase. *Biotechnology and Bioengineering*, 62.2 (1999). 155-159.

20. Migneault, I., Dartinguenave, C., Bertrand, M. J., & Waldron, K. C. Glutaraldehyde: behavior in aqueous solution, reaction with proteins, and application to enzyme crosslinking. *Biotechniques*, 37.5 (2004):790-802.

21. Freeman , A., Abramov, S., & Georgiou, G. Fixation and Stabilization of Escherichia coli Cells Displaying Genetically Engineered Cells Surface Proteins. *Biotechnology and Bioengineering*, 52.5 (1996). 625-630.

22. Gehmlich, I., Pohl, H., & Knorre, W. Laboratory-scale permeabilization of Escherichia coli cells for recovery of a small recombinant protein-Staphylokinase . *Bioprocess Engineering*, 17.1 (1997): 35-38.

23. Kramer, R. A., Brandenburg, K., Vandeputte-Rutten , L., Werkhoven , M., Gros, P., Dekker, N., & Egmond , M. R. Lipopolysaccharide regions involved in the activation of Escherichia coli outer membrane protease OmpT. *European Journal of Biochemistry*, 269.6 (2002): 1746-1752.

24. Kramer, R., Zandwijken, D., Egmond, M. R., & Dekker, N. In vitro folding, purification and characterization of Escherichia coli outer membrane protease OmpT. *European Journal of Biochemistry*, 267.3 (2000):885-893.

25. Bornhorst, J. A., & Falke, J. J. Purification of Proteins Using Polyhistidine Affinity Tags. *Methods of Enzymology*, 326 (2010):245-254.

26. Einhauer, A., & Jungbauer, A. The FLAG peptide, a versatile fusion tag for purification of recombinant proteins. *Journal of Biochemical and Biophysical Methods*, 49.1-3 (2001). 455-465.

27. Schmidt, T. G., & Skerra, A. The Strep-tag system for one-step purification and high-affinity detection or capturing of proteins. *Nature Protocols* , 2 (2007): 1528-1535.

28. Conn, S., Curtin, C., Bézier, A., Franco, C., & Zhang, W. Purification, molecular cloning, and characterization of glutathione S-transferases (GSTs) from pigmented Vitis vinifera L. cell suspension cultures as putative anthocyanin transport proteins . *Journal of Experimental Botany*, 59.13 (2008). 3621-3634.

29. Arca, P., García, P., Hardisson, C., & Suárez, J. E. Purification and study of a bacterial glutathione S-transferase. *Federation of European Biochemical Socities (FEBS)*, 263.1 (1990) 77-79.

30. Novokhatny, V., & Ingham, K. Thermodyamics of maltose binding protein unfolding. *Protein Science*, 6.1 (1997). 141-146.

31. Hewitt, S. N., Choi, R., Kelley, A., Crowther, G. J., Napuli, A. J., & Van Voorhis, W. C. Expression of proteins in Escherichia coli as fusions with maltoe-binding protein to rescue non-expressed targets in a high-throuput protein expression and purification pipeline. *Acta Crystallographica Section F Structural Biology and Crystallization Communications*, 67 (2011). 1006-1009.

32. Jenny, R., Mann, K., & Lundblad, R. A critical review of the methods for cleavage of fusion proteins with thrombin and factor Xa. *Protein Expression and Purification*, 31.1 (2003). 1-11.

33. Hefti, M. H., Van Vugt-Van der Toorn, C. J., Dixon, R., & Vervoort, J. A Novel Purification Method for Histidine-Tagged Proteins Containing a Thrombin Cleavage Site. *Analytical Biochemistry*, 295.2 (2001). 180-185.

34. Guan, K., & Dixon, J. E. Eurkaryotic proteins expressed in Escherichia coli: An improved thrombin cleavage and purification procedure of fusion proteins with glutatione S-transferase. *Analytical Biochemistry*, 192.2 (1991). 262-267.

35. Nilson, B., Morling, F., Cosset, F., & Russell, S. Targeting of retroviral vectors through protease-substrate interactions. *Gene therapy*, 3.4 (1996). 280-286.

36. Renicke, C., Spadaccini, R., & Taxis, C. A Tobacco Etch Virus Protease with Increased Substrate Tolerance a the P1' position. *Public Library of Sciences One*. (2013).

37. Kapust, R. B., & Waugh, D. S. Controlled Intracellular Processing of Fusion Proteins by TEV protease. *Protein Expression and purification*, 19.2 (2000): 312-318.

38. Mao, H., Hart, S., Schink, A., & Pollok, B. A. Sortase-Mediated Protein Ligaqtion: A New Method for Protein Engineering. *Journal of the American Chemical Socieety*, 126.9 (2004): 2670-2671.

39. Cossart, P., & Jonquières, R. Sortase, a universal target for therapeutic agents against Gram-ositive bacteria? *Proceedings of the National Academy of Sciences of the United States of America*, 97.10 (2000): 5013-5015.

40. Breddam, K. Serine Carboxypeptidases. A Review. *Carlsberg Research Communications*, 51.83 (1986): 83-128.

41. Lauritzen, C., Pedersen, J., Madsen , M., Justesen, J., Martensen, P., & Dahl, S. Active recombinant rat dipeptidyl aminopeptidase I (cathepsin C) produced using the baculovirus expression system. *Protein Expression and Purification*, 14.3(1998). 434-42.

42. Zamora, D., Natesan, S., & Christy, R. Constructing a Collagen Hydrogel for the Delivery of Stem Cell-loaded Chitosan Microspheres. *Journal of Visualized Experiments*. 64 (2012).

43. Pédelacq, J.-D., Cabantous, S., Tran, T., Terwilliger, T., & Waldo , G. Engineering and characterization of a superfolder green fluorescent protein. *Nature Biotechnology*, 24.1(2005):79-88.

44. Lim, L., Wan, L. S., & Thai, P. Chitosan Microspheres Prepared by Emulsification and ionotropic gelation. *Drug Development and Industrial Pharmacy*, 23.10 (1997): 981-985.

45. Grisshammer, R., & Tucker, J. Quantitative Evaluation of Neurotensin Receptor Purification by Immobilized Metal Affinity Chromatography. *Protein Expression and Purification*, 11.1 (1997): 53-60.

46. Wan, L., Heng, P., & Chan , L. Drug encapsulation in alginate microspheres. *Journal of microencapsulation*, 9.3 (1992): 309-316.

47. Kildeeva, N., Perminov, P., Vladimirov, L., Novikov, V., & Mikhailov, S. About Mechanism of Chitosan Cross-Linking with Glutaraldehyde. *Russian Journal of Bioorganic Chemistry*, 35.3 (2009) 360-369.

48. Cayot, P., & Tainturier, G. The quanitfication of protein amino groups by the trinitrobenzenesulfonic acid method: a rexamination. *Analytical Biochemisry*, 249.2 (1997): 184-200.

49. Shi, Q., Tian, Y., Dong, X., Bai, S., & Sun, Y. Chitosan-coated silica beads as immobilized metal affinity support for protein adsoprtion. *Biochemical Engineering Journal*, 16.3 (2003): 317-322.

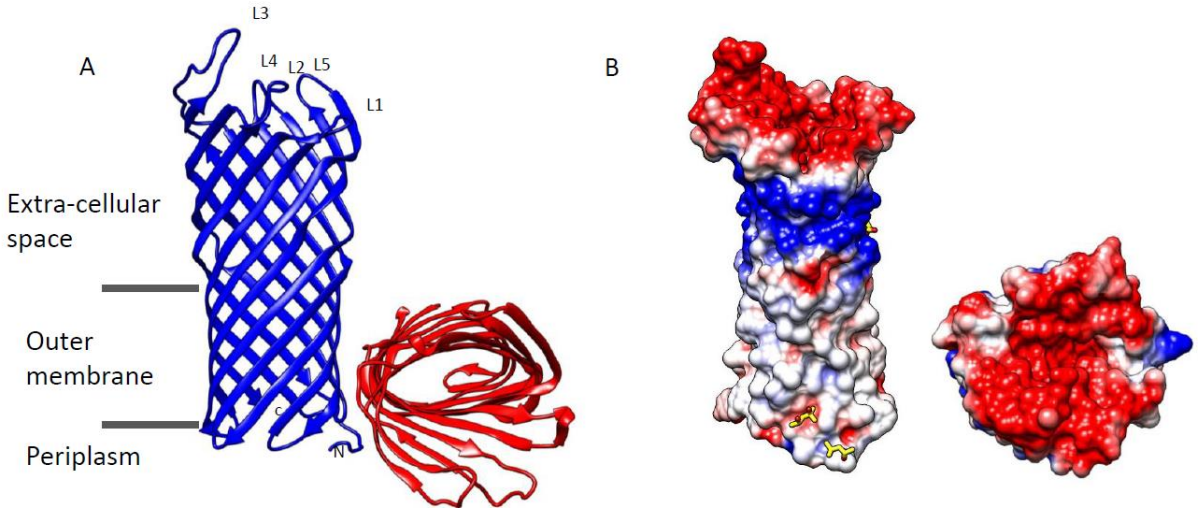

Figure 1: Overall structure of OmpT. A) Vertical and horizontal ribbon (respectively) representation of OmpT depicting locations of the protein within the extra-cellular space, outer membrane, and in the periplasmic region. Extracellular loops are labelled L1-L5. B) Electrostatic potential of a cross section of the β-barrel of OmpT. Negative charges are labeled in red, positive charges in blue, and neutral/hydrophobic regions in white. All molecular graphics and analyses were performed with the UCSF Chimera package. Chimera is developed by the Resource for Biocomputing, Visualization, and Informatics at the University of California, San Francisco (supported by NIGMS P41-GM103311)

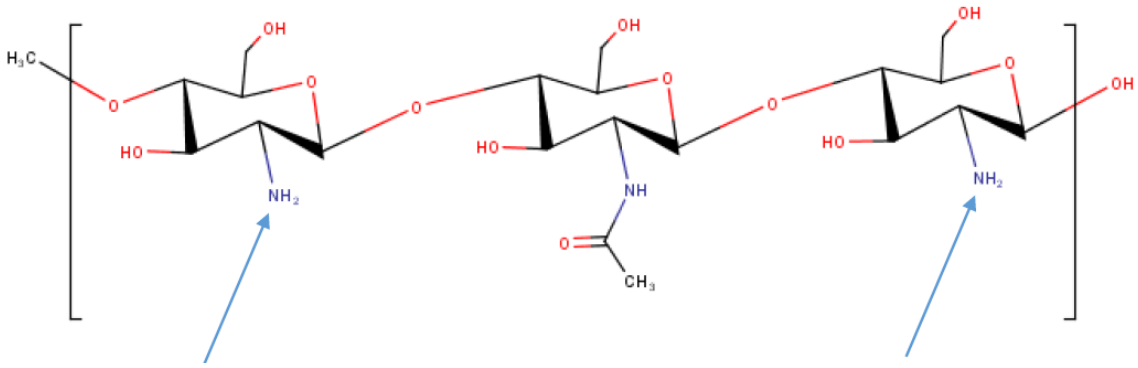

Figure 2: A) Molecular depiction of chitosan. Amine-groups, as pointed out, are areas of catalytic exchange between either anions or fixatives such as glutaraldehyde. Amine groups have a pKa of the amine group ~6.5. Sites of fixative attachment are defined.

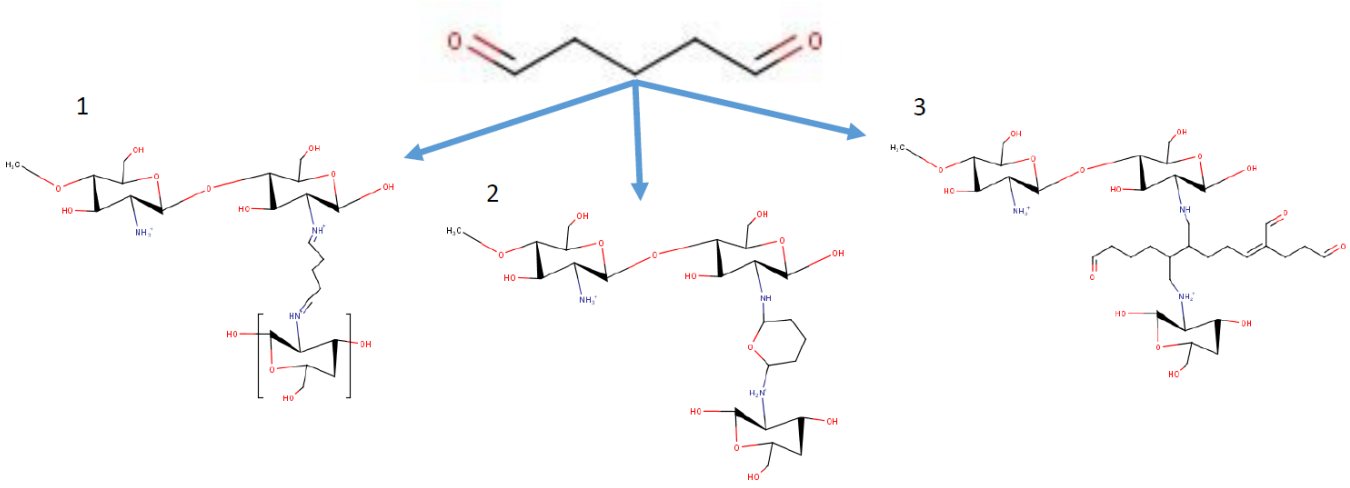

Figure 3: Glutaraldehyde. Skeletal formula of glutaraldehyde and its conjugates with chitosan with 1) Schiff base formation, 2) polymeric glutaraldehyde under acidic conditions, and 3) polymeric glutaraldehyde under basic conditions. Though there are many possible conformations of glutaraldehyde/chitosan conjugates, the ones shown are just a few of them [19].

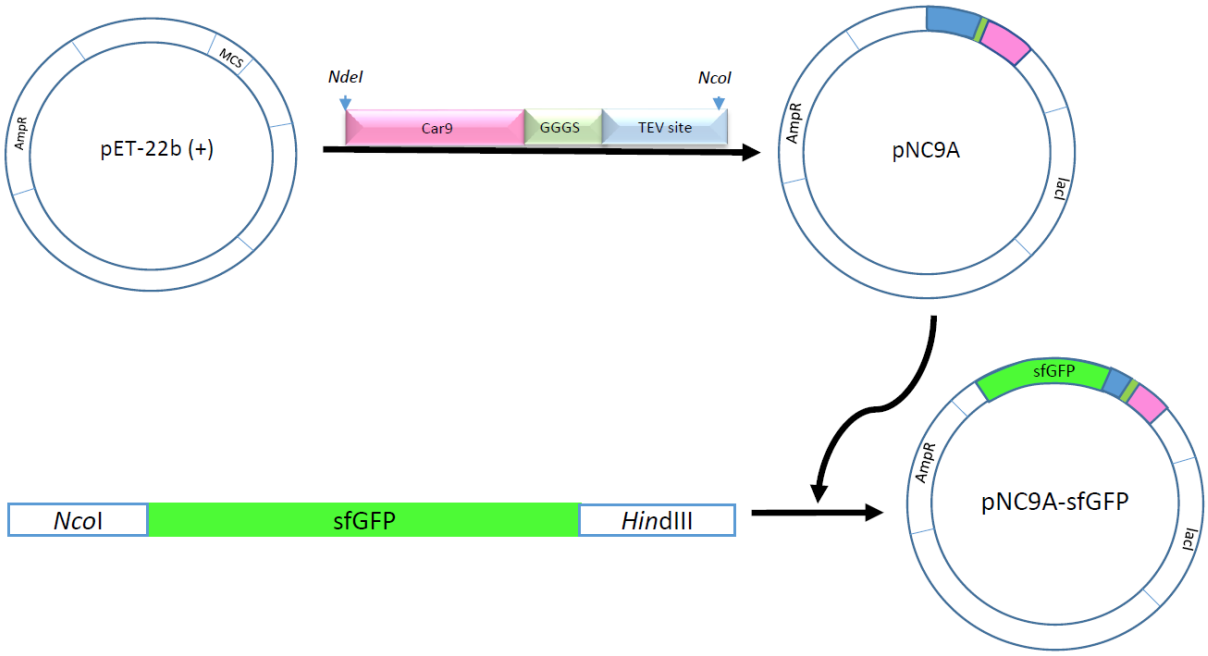

Figure 4: DNA manipulation to produce N-terminal Car9 and Car9-sfGFP. A 100 bp DNA cassette containing a Car9 tag and TEV protease site with a GGGS linker and *NdeI* and *NcoI* (5'-CGTATACATATGGGCAGCAGCGACAGTGCTCGCGGGTTTAAAAAGCCTGGGAAGCGGGGCGGCGGCTCTGAAAACTTATACTTCCAGTCCATGGTATACG-3')is inserted into a blank pET-22b(+) vector (Novagen). Afterwards, sfGFP from pET-24a(+) is amplified with *NcoI* and *HindIII* sites using PCR. Then, the sfGFP is inserted into NC9A using NcoI-HindIII cuts to produce Car9-sfGFP.

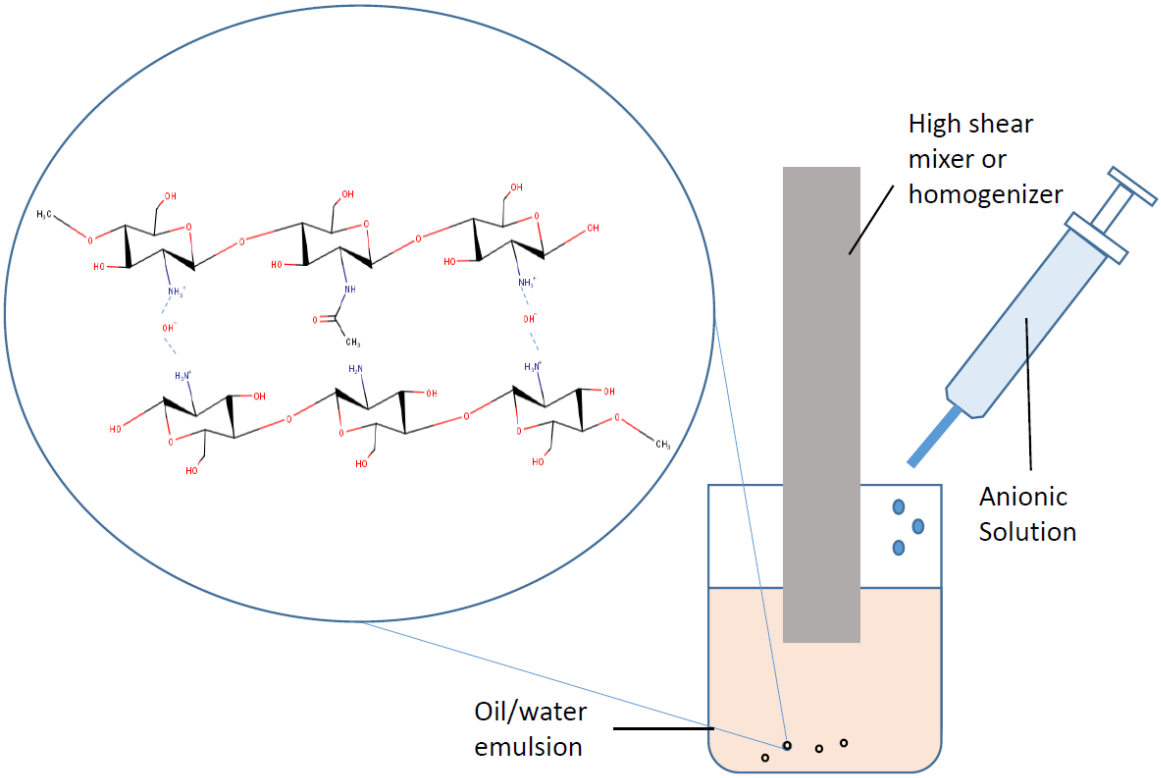

Figure 5: Process of ionotropic gelation. Dissolved polymeric chitosan is added to an oil solution (1:1 octanol/paraffin oil) supplemented with emulsifier, Span 85, and homogenized, forming a water/oil emulsion. Afterwards, an anionic solution either 1 wt% potassium hydroxide in butanol is added at increments of 15 minutes for 4h. Molecular structure of chitosan after ionotropic gelation is shown.

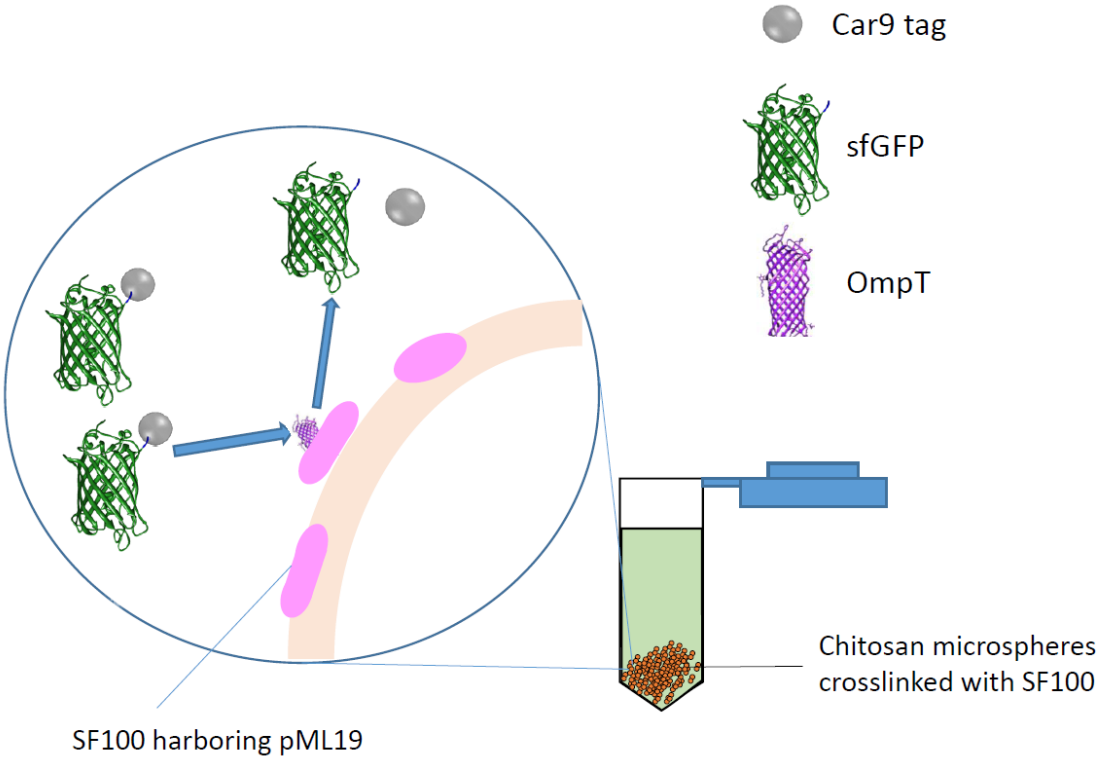

Figure 6: Conceptual design for chitosan microsphere cleavage. Chitosan microspheres are crosslinked with SF100 containing pML19, overexpressing OmpT, using glutaraldehyde. These crosslinked/immobilized cells surface-exposed OmpT to cut at appropriate positions of sfGFP-Car9, removing the Car9 tag. Both tag and native protein are free in solution for further processing.

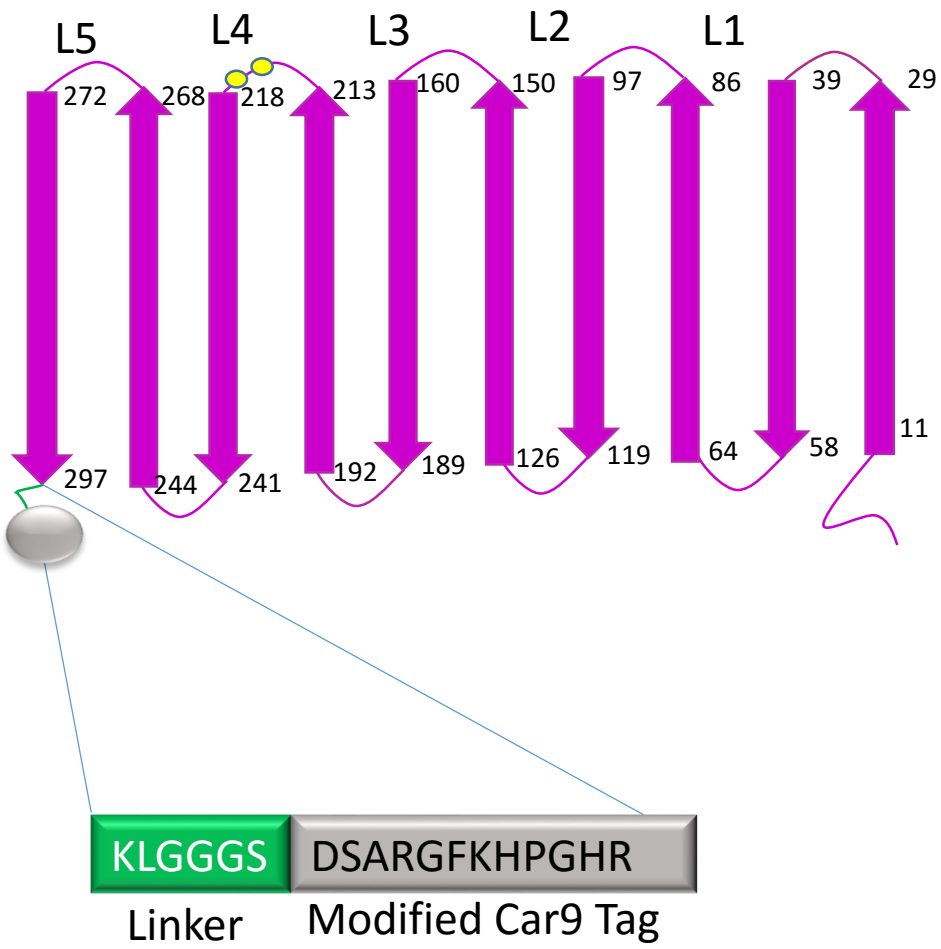

Figure 7: Cartoon structure of OmpT- K8H/K11H Car9 showing location and amino acid composition of Car9 as well as locations of the K216G/G217K mutations to prevent autocatalytic activity (yellow circles).

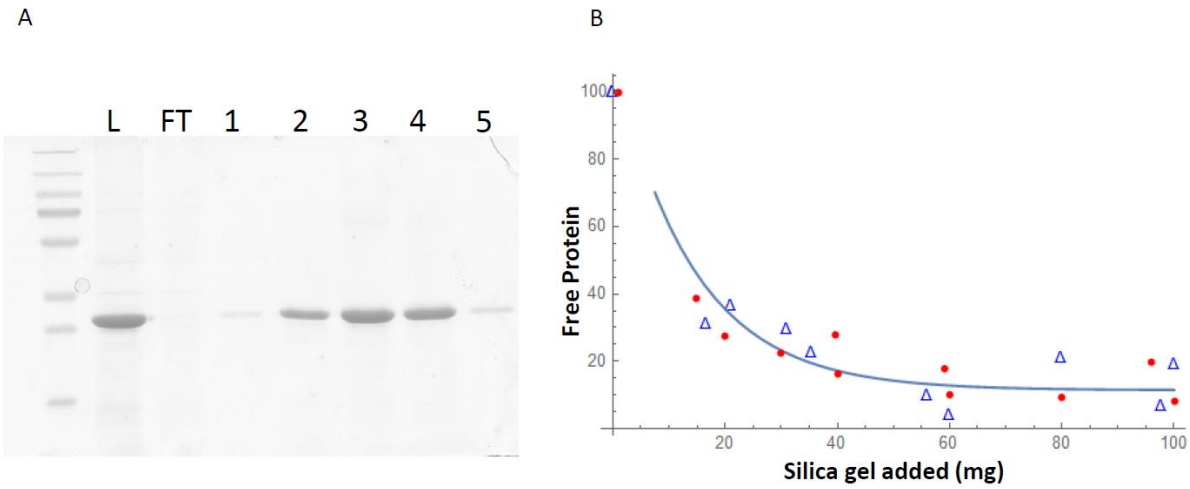

Figure 8: Car9-sfGFP analysis. A) SDS-PAGE analysis of the rapid purification process using silica. L is the load of cell lysate post-processing. FT is the flow through. 1-5 are each elution fraction. B) Analysis of protein-silica interactions using fluorescence depletion assay on N terminally (Δ) and C terminally (●) tagged proteins. Both follow a trendline, $100*e^{(-.07121x)}$ reducing the sum of squared error on an exponential regression.

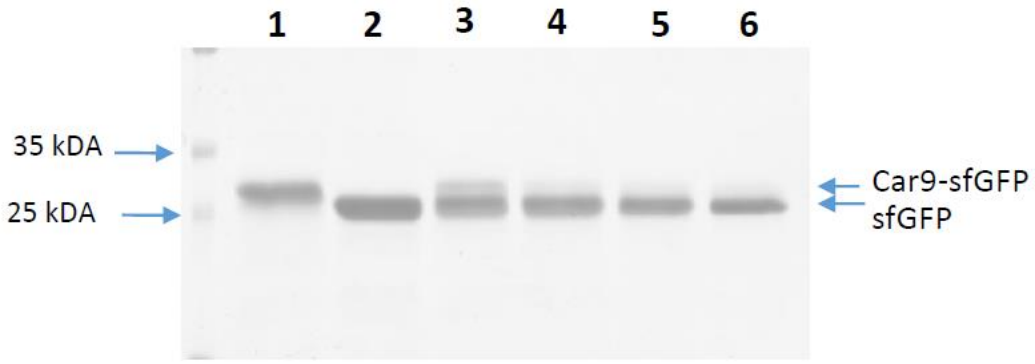

Figure 9: SDS-PAGE analysis of TEV cleavage of Car9-sfGFP. 14 µg of Car9-sfGFP incubated with 10 units of TEV protease. Lanes: 1) Car9-sfGFP, 2) sfGFP, 3) 12h incubation, 4) 36h incubation, 5) 72h incubation, and 6) 96h incubation. Arrows indicate migration position of Car9-sfGFP to sfGFP respectively.

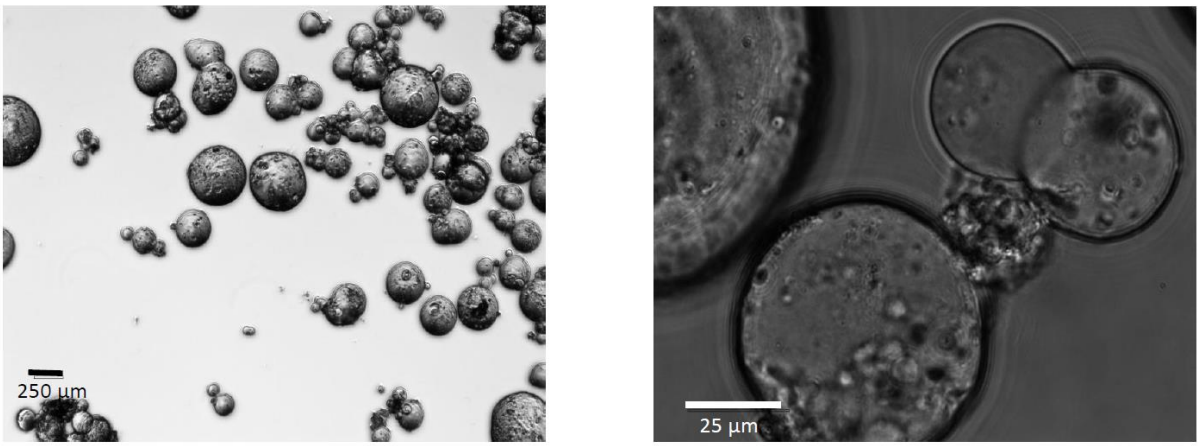

Figure 10: Chitosan microspheres formed using ionotropic gelation in an oil/water emulsion. Distinct rigid microspheres were formed >80% ranging from 50-150 µm diameter with minor spherical malformations. Images were attained using a contrast microscope on bright field.

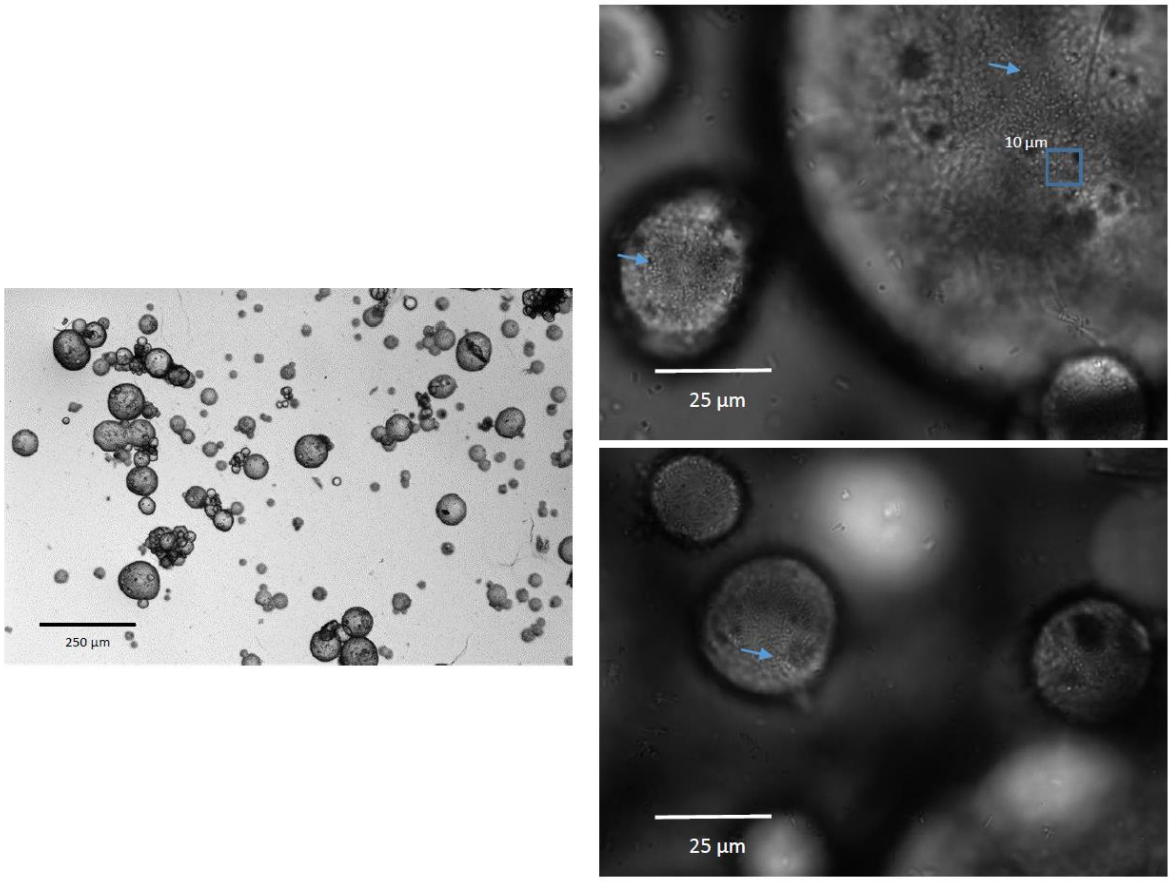

Figure 11: Crosslinking onto chitosan microspheres. SF100 cells harboring pML19 were first fixated using glutaraldehyde then incubated with chitosan microspheres. A) shows a macroscopic view of the chitosan spheres at 4X in bright field, while B) shows the chitosan spheres at 90X in bright field. Crosslinked *E. coli* can be seen in densely packed sections of the sphere, averaging 20 cells in a 10 µm square.

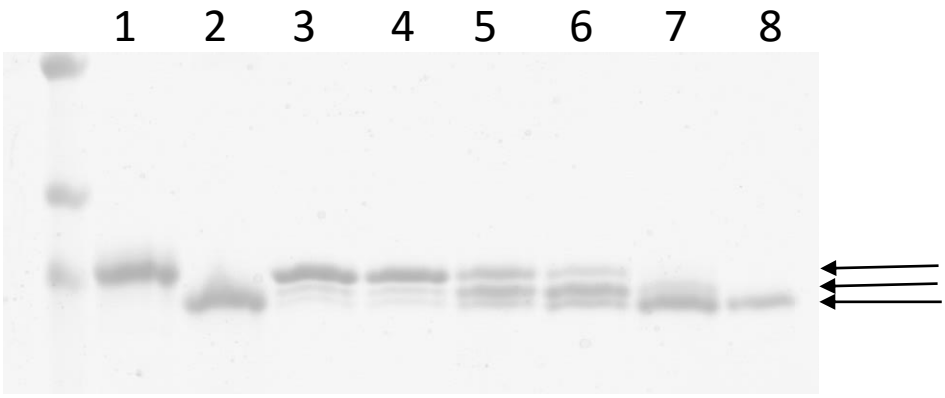

Figure 12: SDS-PAGE of the Car9 excisions using chitosan microspheres coated in SF100 harboring pML19. The lanes are as follows: 1) Negative control sfGFP-Car9, 2) positive control sfGFP, 3) 30-min incubation, 4) 1 hr incubation, 5) 3-hr incubation, 6) 6-hr incubation, 7) 16-hr incubation, 8) 24-hr incubation. Three distinct bands are visible with increasing incubation. The first band indicates sfGFP-Car9 fusion, the second band indicates a transitionary cut within the Car9 tag, and the third band migrates towards sfGFP indicating a full excision within 24 hr.

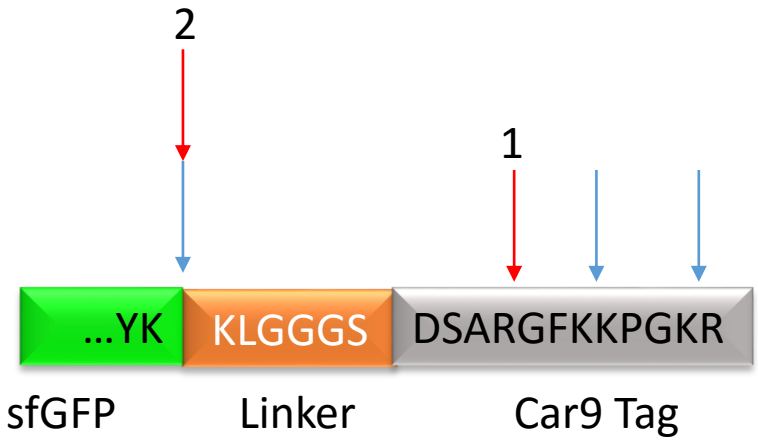

Figure 13: Sites of OmpT cleavage on the C-terminal Car9 tag fused to sfGFP. Blue arrows depict cleavage patterns as expected in [3]. Red arrows depict cleavage patterns as predicted by [11]. Dekker's excision positions [11] were found more favorable as the excised molecular weights are .98 (1) and 1.8 (2) respectfully.

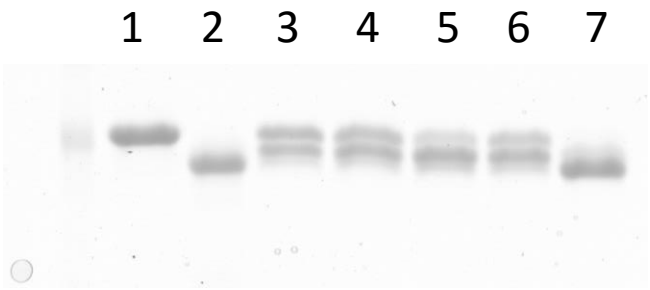

Figure 14: SDS-PAGE of the Car9 excisions **using previously used** chitosan microspheres coated in SF100 harboring pML19. The lanes are as follows: 1) Negative control sfGFP-Car9, 2) positive control sfGFP, 3) 30-min incubation, 4) 1-hr incubation, 5) 3-hr incubation, 6) 6-hr incubation, 7) 16-hr incubation. No apparent decrease in catalytic efficiency is noticeable after multiple runs.

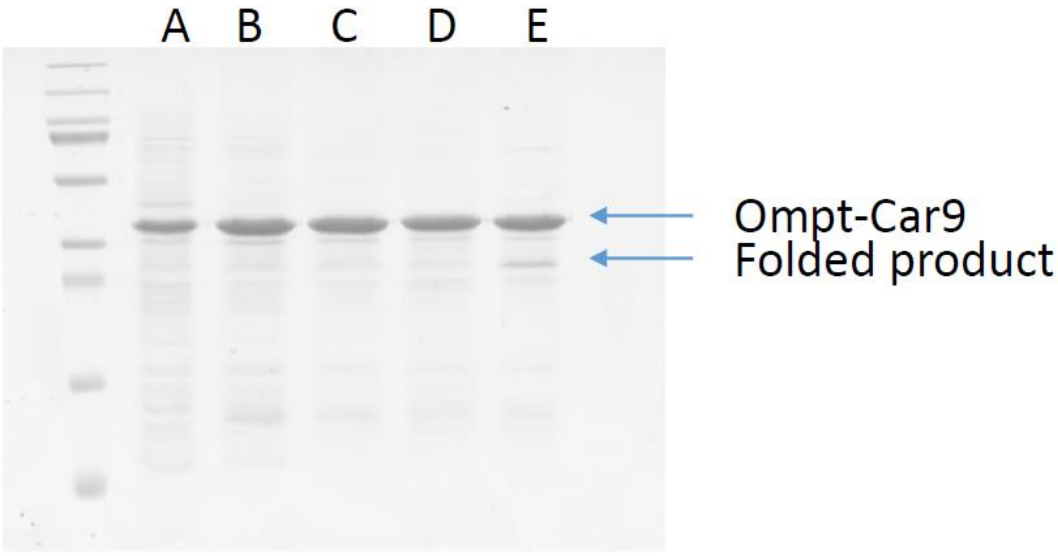

Figure 15: OmpT-Car9 inclusion bodies and washing steps. A) Whole-cell sample BL21DE3 cells 6h after induction with 1 mM IPTG at A_{600} ~ .4. B) Sample after lysis using Branson sonicator and incubated with lysozyme. C) Inclusion bodies centrifuged down, resuspended, and sonicated, D) twice. E) Sample after unfolding, refolding, and incubation with 1 µg/mL lipopolysaccharides. OmpT-Car9 is found at around 35.3 kdA. Folded OmpT-Car9 band is found to migrate at a lower kDa due to structural conformation.

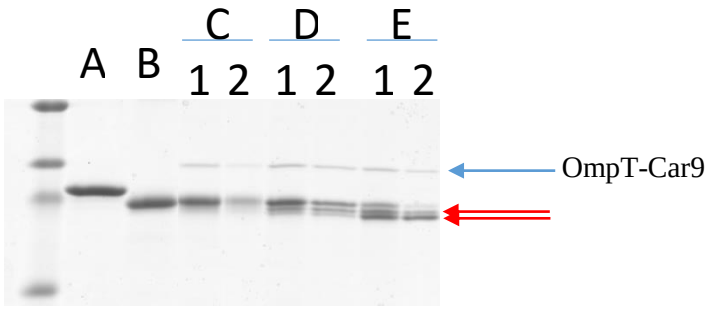

Figure 16: OmpT-Car9 cleavage **prior to detergent removal**, a time trial. 2 µg of OmpT-Car9 was incubated with 50 µL of 10 µM sfGFP-Car9. Lanes are as follows: A) sfGFP-Car9. B) sfGFP. C) 3-hr incubation D) 6-hr incubation E) 16-hr incubation. (1) are the bands prior to silica incubation. (2) are the bands after a 15 min incubation with 10 µL of silica slurry (~60 mg silica gel). Red arrows indicate the initial and final cleavage products while the blue arrow shows the band for OmpT-Car9.

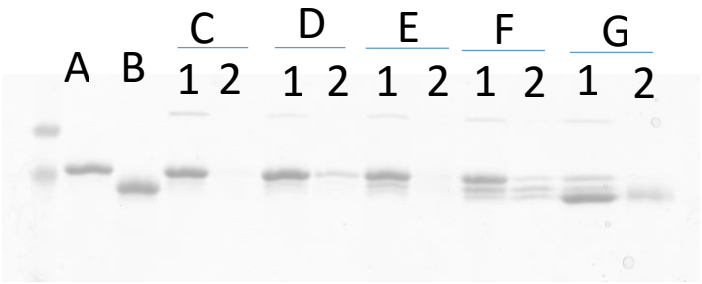

Figure 17: OmpT-Car9 cleavage **after detergent removal with dialysis**, a time trial. 1 µg of OmpT-Car9 was incubated with 50 µL of 10 µM sfGFP-Car9. Lanes are as follows: A) sfGFP-Car9, B) sfGFP, C) 1-hr incubation, D) 3-hr incubation, E) 6hr incubation, F) 16-hr incubation, G) 24-hr incubation. (1) are the bands prior to silica incubation. (2) are the bands after a 15-min incubation with 10 µL of silica slurry.

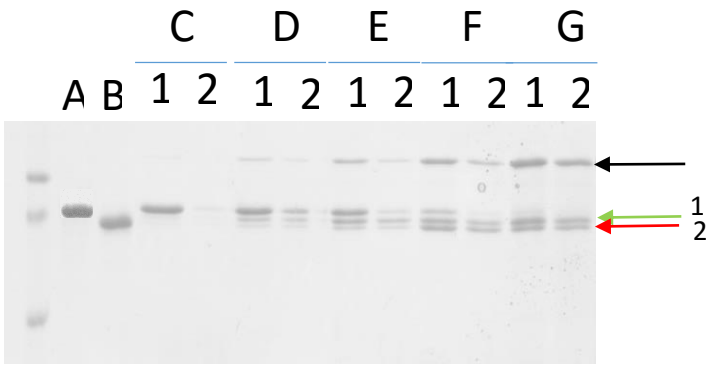

Figure 18: OmpT-Car9 cleavage and cleavage sites. 1-50 µg of OmpT-Car9 incubated with 100 µL of 10µM sfGFP-Car9. Lanes are as follows: A) sfGFP-Car9. B) sfGFP. C) 1 µg of OmpT-Car9. D) 5 µg of OmpT-Car9. E) 10 µg of OmpT-Car9. F) 20 µg of OmpT-Car9 G) 40 µg of OmpT-Car9. (1) are the bands prior to silica incubation. (2) are the bands after 15 minutes of silica incubation. Yellow arrow shows sfGFP-Car9 fusion protein. Black arrow depicts OmpT-Car9. Red and green arrows depict cleavage sites on the Car9/linker.

Table 1: Common affinity tags.		
Affinity tags	Amino acid sequence - kDA	References
6X Histidine Tags	$(H)_6$ - .84	24
FLAG	DYKDDDDK- 1.01	25
Strep-Tag II	WSHPQFEK – 1.06	26
Glutathione S-transferase	Protein - 26	27,28
MBP	Protein - 40	29,30

Table 2: Popular proteases for tag removal. * denotes site of cleavage. X is an unspecified amino acid			
Proteases		Cleavage Site	References
Endoproteases			
	Thrombin	LVPR*GS	31, 32, 33
	Factor Xa	IDGR*X…	31, 34
	TEV Protease	EQLYFQ*G	35, 36
	Sortase A	LPET*GXX	37, 38
Exoproteases			
	Carboxypeptidase A		39
	Carboxypeptidase B		
	DAPase		40

Supplementary Material

I. Chitosan microsphere formation was adapted from Patil's review [17]. Chitosan is first dissolved in 2% vol/vol acetic acid to make a 2.5% wt/vol solution. 10 mL of the solution was added to 75 mL of paraffin oil or heptane supplemented with 2% wt/vol Span 85 emulsifier (Sigma) in a baker. The mixture was subjected to 1000-5000 rpm agitation using a Ross homogenizer. After 15 minutes of emulsification, 2 M sodium hydroxide was added dropwise at a rate 5 mL/30 min for 90 min using a simple peristaltic pump. The mixture was then allowed to stir for an additional 15 minutes. The oil phase was removed and discarded, and the chitosan microspheres were washed repeatedly with 1X PBS buffer (50 mL) until the supernatant was neutral and clear.

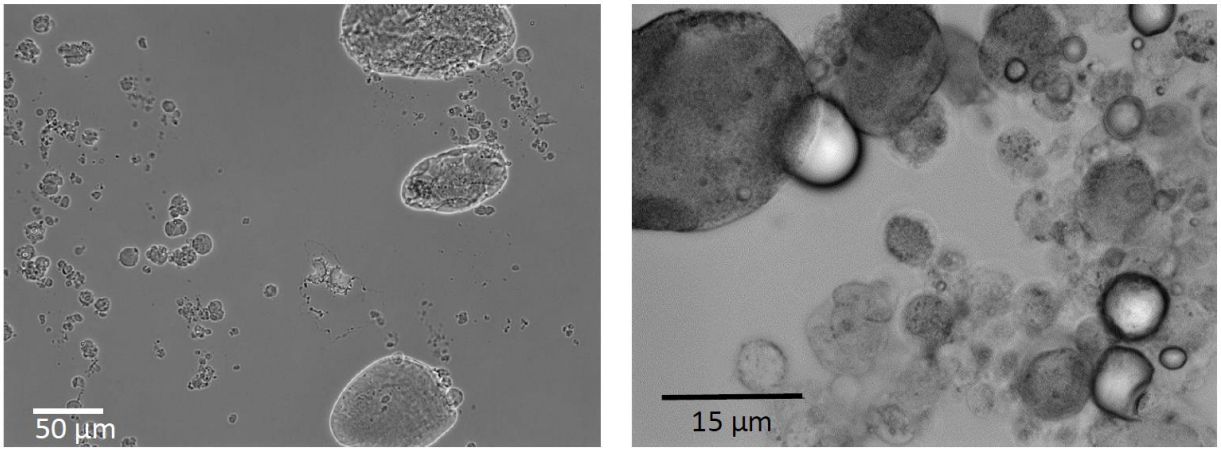

Figure S1: Microspheres made from protocol adapted from Patil, Chavanke, and Wagh. Particles formed were either distributed in large aggregates or displayed structures that were easily deformable. The method and resulting microsphere formations were inconsistent, low yielding, and lacked rigidity, which was not conducive for further application in crosslinking with SF100 harboring pML19.

II. Another method of chitosan microsphere formation was adapted from Nomanbhay and his coworkers [16]. Chitosan is first dissolved in 2% vol/vol acetic acid to make a 2.5% wt/vol solution. 10 mL of the solution was added dropwise using a simple peristaltic pump into a large bath of 2 M sodium hydroxide (50 mL) under agitation from a magnetic stir rod. Microspheres were then allowed to incubated under agitation for 12h before filtered and washed thoroughly with ddH_2O. Microspheres were stored in ddH_2O at room temperature.

III. Chitosan coated silica particles

a. Method: Silica (200-420 mesh, 150A pore purchased from Sigma Aldrich), 2 g, is first washed with ddH_2O and incubated in 100 mL of 20% HCL for 16 h at room temperature with constant agitation from a magnetic stir-bar. The supernatant was discarded and the silica was washed 5 times with ddH_2O to remove any HCL content. Next, 10 mL of chitosan solution consisting of 2.5% (wt/vol) of medium molecular weight chitosan (Sigma) in 2% (v/v) acetic acid was added to the silica and the mixture was stirred for another 12 h on a stirring plate and allowed to settle for an additional 48 h. The supernatant was then removed and discarded and the chitosan-coated silica particles were washed with water 5 times with 50 mL ddH_2O . The particles were then resuspended in 100 mL of ddH_2O. The pH was brought up to 9 using 1M NaOH and was agitated on a stir plate for 2h to coat and fix chitosan onto the silica particles. The particles were again decanted and washed with ddH_2O and taken in 200 mL of 0.01% (v/v) glutaraldehyde in ddH_2O for 16 h [49]. The particles were washed with distilled water and 10% ethanol to remove any additional glutaraldehyde.

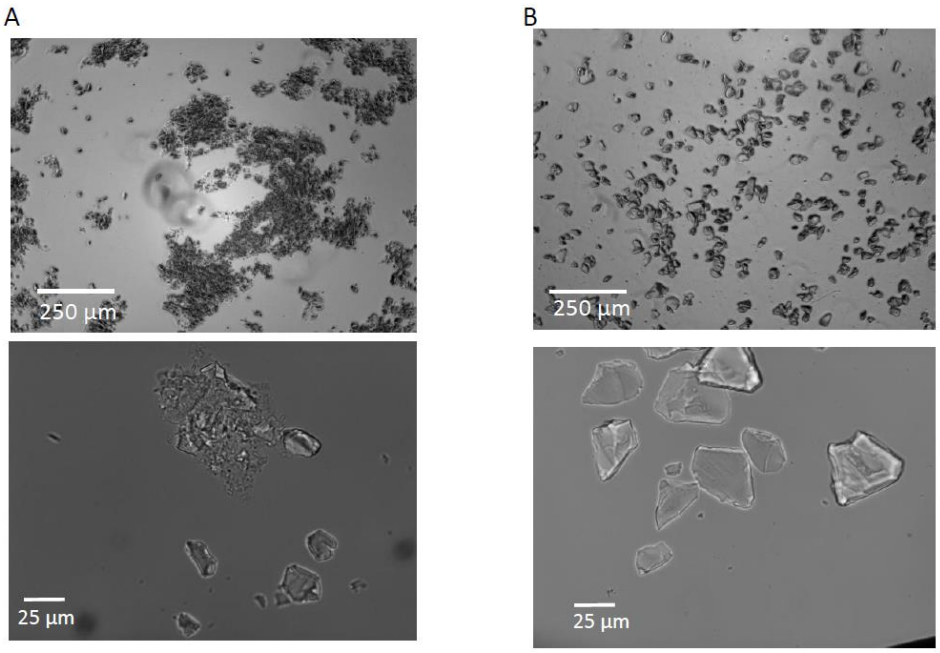

Figure S2: Chitosan coated silica particles. A) Images of silica particles after chitosan coating using glutaraldehyde at Mesh (200-420) and B) of silica microparticles (Mesh 200-420) at both 4X and 90X magnification in bright field. Coated silica is visible as well as chitosan aggregates forming around multiple silica particles. Some silica particles appear uncoated or without full coverage.

IV. SF100 immobilized onto chitosan coated silica particles

SF100 cells fixated with .2% glutaraldehyde were added to .2 g of chitosan coated silica particles for 24h.

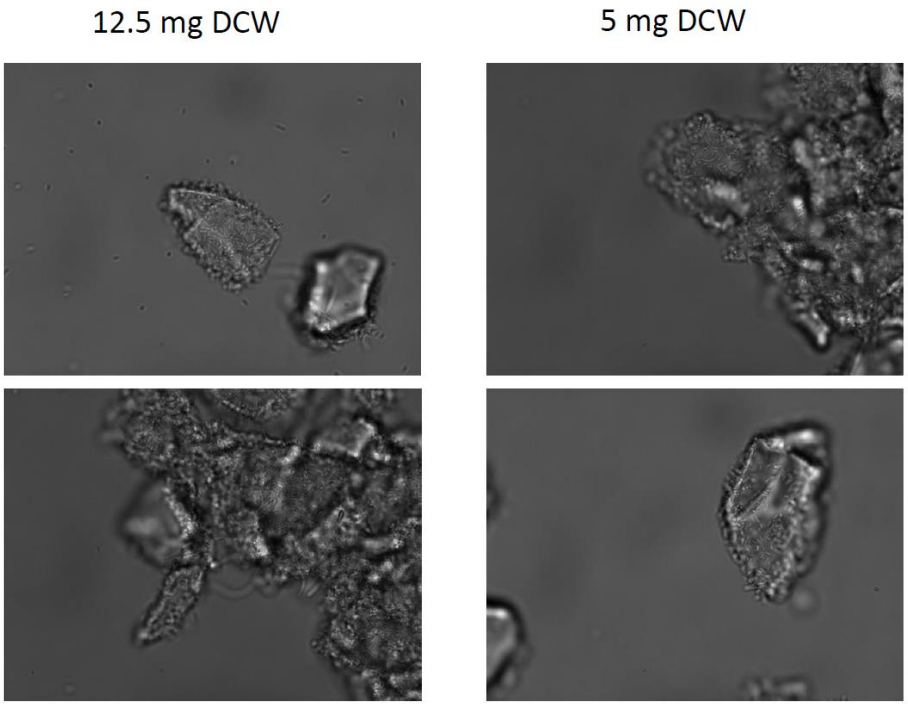

Figure S3: SF100 harboring pML19 crosslinked onto chitosan coated silia particles after fixation using glutaraldehyde. The left column shows 12.5 mg DCW cells added to 200 mg of chitosan coated silica particles while the right column shows 5 mg DCW added to 200 mg chitosan coated silica particles. Both reveal coverage with some minor cellular debris in the background, which is resolved through extensive washes. Further use of for Car9 excision were proven difficult as the Car9 tagged protein were selectively attaching to exposed silica even with elution conditions. Use of chitosan coated silica with crosslinked SF100 harboring pML19 was unadvisable due to this occurrence.

V. Glutaraldehyde crosslinked cells

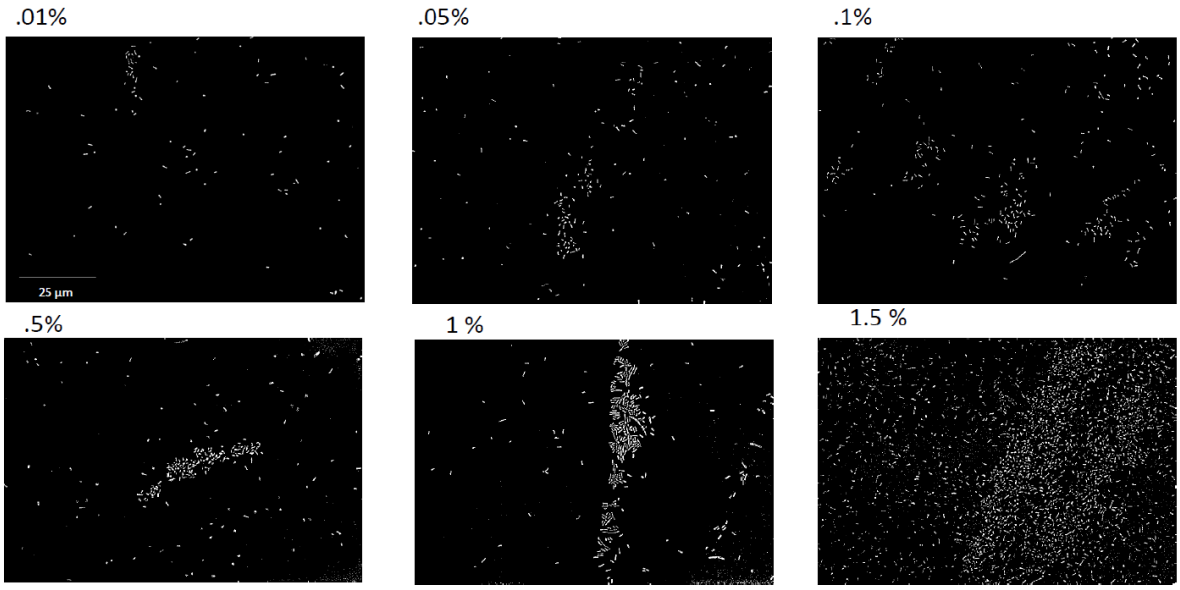

Figure S4: Glutaraldehyde cross-linked E.coli cells ranging from .01% to 1.5% v/v. **Increasing glutaraldehyde concentration increases *E. coli* cell cross linking.** Glutaraldehyde concentrations vary from 0.1% to 1.5% during an overnight incubation. Cells are imaged at 90x in bright field. Images were adjusted to display cross-linking. Adjusted images show crosslinking occurring, but majority of cells remained in solution. This finding along with another showing aggregates at any % of glutaraldehyde as in 1% reveal that the crosslinking efficiency of whole cells onto whole cells is limited.

VI. OmpT-Car9 production with un-boiled sample.

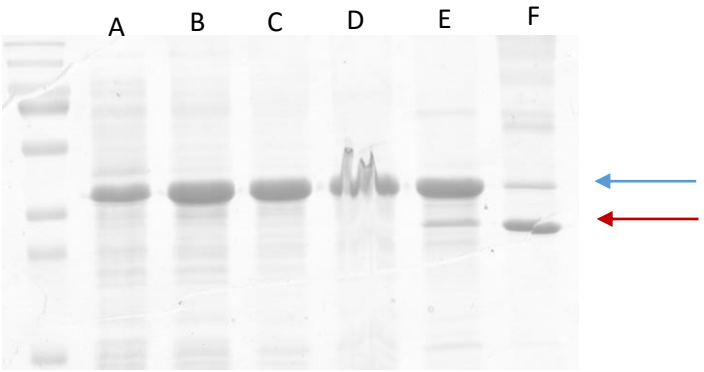

Figure S5: A) Whole-cell sample BL21DE3 cells 6h after induction with 1 µM IPTG at OD .4. B) Sample after lysis using Branson sonicator and incubated with lysozyme. C) Inclusion bodies centrifuged down, resuspended, and sonicated, D) twice. E) Sample after unfolding and refolding and after incubation with 1 µg/mL lipopolysaccharides, which is boiled for 10 minutes. F) Un-boiled sample incubated with loading buffer from Lane E).

VII. Chitosan microsphres following the same protocol as Material Methods IV but using 2% Span 85 instead.

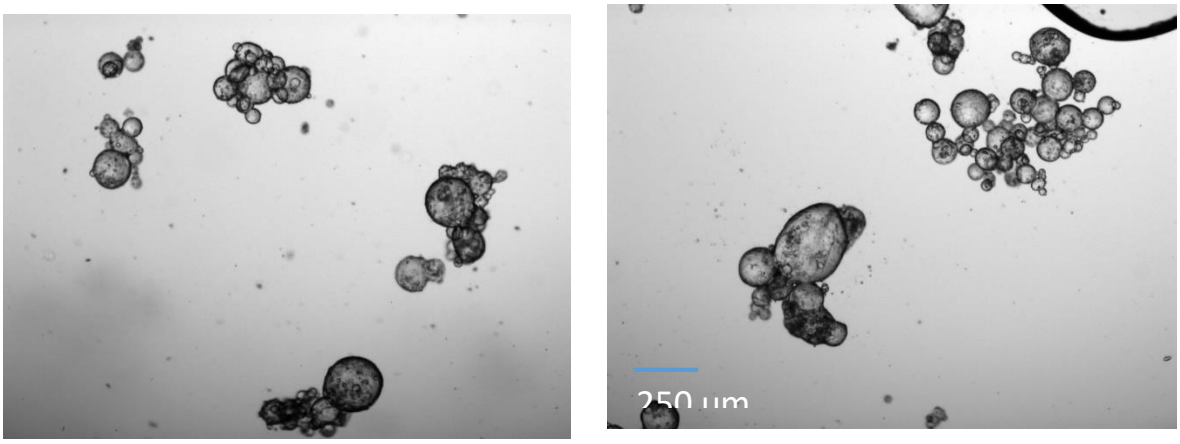

Figure S6: Chitosan microspheres formed using 2% Span 85 following Materials and Methods IV. Chitosan microspheres were found mainly as aggregated spheres than distinct spherical formations.

VIII. BCA analysis of OmpT-Car9 binding affinity

In order to assess the binding affinity of OmpT-Car9, aliquots of refolded OmpT-Car9, sfGFP-Car9, and sfGFP-Car9 incubated with LPS were added to 30 and 100 μL silica slurry or ~60 mg of silica gel. The results shown on Table S1 reveal that OmpT-Car9 has a significant reduction of binding capacity in comparison to sfGFP-Car9. This may be attributed to the incubation with LPS and the position by which the Car9 is appended to OmpT.

Table S1 also shows a reduction in Car9 binding between sfGFP-Car9 and sfGFP-Car9 incubated in LPS by 11% [Table S1]. On OmpT, LPS bound to the periphery of the beta-barrel within the section secluded to the outer-membrane, but are known to bind to OmpT along residues Arg138, Arg175, Lys226, Glu136 and Tyr134 [13]. Similarly, the Car9 binding peptide as well relies on its basic residues, arginine and lysine, as well as hydrophobic residues, phenylalanine and alanine, to bind to silica [3]. Therefore, the decrease in binding efficiency between sfGFP-Car9 and sfGFP-Car9 incubated with LPS may be attributed to the competitive binding of LPS onto Car9 prior to Car9-silica interaction [Table S1]. Though the change in binding efficiency with LPS incubation is significant, OmpT-Car9's lowered affinity to silica cannot be explained with just LPS incubation.

The Car9 tag placement on the C-terminus also was a valid concern because the C-terminal region of OmpT may have sterically hindered the Car9 tag's binding range due to its close proximity with the beta-barrel [13]. Unlike OmpT, sfGFP has its C and N terminal regime further from the beta barrel allowing the Car9 to be free for binding opportunity [Figure S7]. As indicated by the black circles on Figure 19, OmpT's C-terminus contains nearby negative charges which also may effect binding affinity towards silica. This may explain why even when compensating for LPS, OmpT-Car9's binding capacity is significantly lower than that of sfGFP-Car9. Moving the Car9 tag to a more exposed region of the protein such as the N-terminus or within a periplasmic loop of OmpT may increase Car9 binding efficiency.

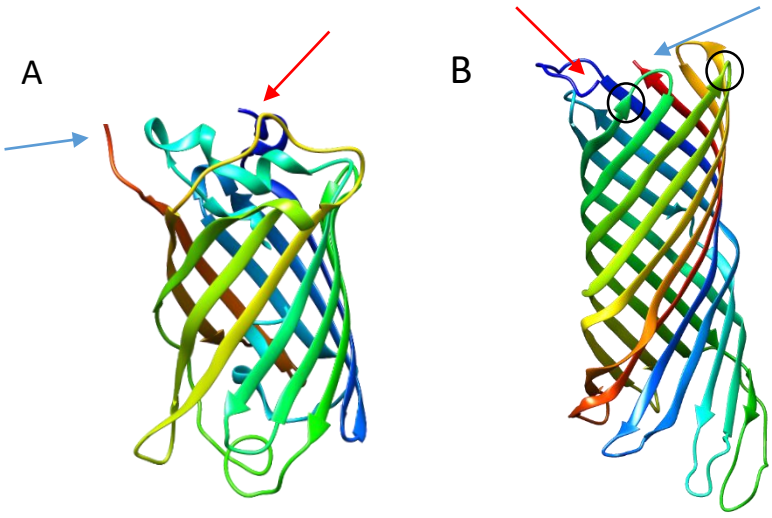

Figure S7: Crystal structures of both sfGFP (A) and OmpT (B). N-termini are depicted with red arrows while C-termini are depicted in blue arrows. The C-terminal regime on OmpT where the Car9 tag is placed is at end of the beta-barrel flanked by periplasmic turns. The N-termini of OmpT is found to be more free, protruding out of the beta barrel. sfGFP has both of its termini protruding from the beta-barrel, allowing the fused Car9 tag to bind freely. Black circles indicate negatively charged residues near the C-terminus on OmpT.

Table: S1: OmpT-Car9 binding capacity on silica in comparison to sfGFP-Car9 and sfGFP-Car9 incubated with LPS after incubation for 15 minutes.

Sample	Total Protein (µg)	Total desired protein (µg)	µL slurry added	Protein bound (µg)	% of binding capacity
OmpT-Car9	146	117	0	0	NA
	116.8	92	30	25	20
	68	54	100	62	16
sfGFP-Car9	347		0	0	NA
	241		30	106	88
	147		100	199	50
sfGFP-Car9 with 1 µg/mL LPS	339		0	0	NA
	248		30	91	76
	183		100	156	39